SOME PHYSICO-CHEMICAL PROPERTIES OF AMORPHOUS MINERAL COLLOIDS

A THESIS SUBMITTED TO THE GRADUATE DIVISION
OF THE UNIVERSITY OF HAWAII
IN PARTIAL FULFILLMENT OF THE
REQUIREMENTS FOR THE DEGREE OF

MASTER OF SCIENCE

IN SOIL SCIENCE

JANUARY 1967

By

Sung-ho Lai

Thesis Committee:

Dr. Leslie D. Swindale, Chairman
Dr. J. Adin Mann
Mr. Haruyoshi Ikawa

We certify that we have read this thesis and that in our opinion it is satisfactory in scope and quality as a thesis for the degree of Master of Science in Soil Science.

THESIS COMMITTEE

H. B. Swindale
Chairman

J. Odin Mann, Jr.

Haruyoshi Ikawa

ACKNOWLEDGMENT

The author is indebted to the East-West Center for financial aid received during this project. Appreciation is extended to the Department of Chemistry and Department of Microbiology for the use of their facilities.

The author wishes to thank Mr. S. Pandey for running multiple regressions, Mr. G. Tsuji for drawing and Misses Sandra Yee, Judy Kimura and Karen Nishimoto for helping in the preparation of the manuscript. Thanks are also extended to other graduate students of the Department of Agronomy and Soil Science for their friendship and encouragement which made his stay at the University more meaningful and enjoyable.

ABSTRACT

The amorphous mineral colloids were separated by the particle size method from four Hawaiian soils and a Japanese soil known to have high contents of these colloids. These five soils represent weathering conditions ranging from moderately to strongly weathered, with varying silica-alumina ratios.

The physico-chemical properties of amorphous mineral colloids were studied by several methods: X-ray diffraction analysis, differential thermal analysis, elemental analysis, electron microscopy, infrared absorption spectroscopy, surface area determination, and cation exchange capacity determination.

The fine clay fraction (less than 0.1 μ) was x-ray amorphous with various amounts of weakly formed 2:1 minerals. The coarse clay fraction consisted mainly of the crystalline minerals mica, kaolin, and gibbsite. From DTA patterns it was found that the first endothermic reaction was closely related to the degree of crystallinity estimated from the x-ray data.

The silica-alumina molar ratios were within the range of 0.927 to 1.940, and the loss on ignition was found to be inversely proportional to the silica-alumina ratio.

The micromorphology of the fine fraction as examined under the electron microscope showed fibrous and sponge-like features. The fibrous material decreases with an increasing degree of crystallinity. The morphology of the coarse fraction, however,

changes as the degree of crystallinity increased, from irregularly-shaped flakes to pseudohexagonal flakes, accompanied by an increase in the size of the flakes and a decrease in the amounts of fibrous and sponge-like material.

The main infrared absorption band at 10 μ shifted from 9.75 to 10.3 μ as the $Al_2O_3/(Al_2O_3+SiO_2)$ weight ratio increased from 50% to 65% reflecting the change in the coordination state.

The surface area determinations were inconsistent with observations made of clay specimens with the aid of the electron micrograph.

The CEC increased with increasing pH, increasing more rapidly when alkaline. The ΔCEC increased curvilinearly with the $Al_2O_3/(Al_2O_3+SiO_2)$ weight ratio from 45% to 65%. This may be attributed to the strong acid behavior of Al^{IV}.

TABLE OF CONTENTS

TABLE OF CONTENTS (Continued)

TABLE OF CONTENTS (Continued)

LIST OF TABLES

LIST OF FIGURES

LIST OF FIGURES (Continued)

LIST OF FIGURES (Continued)

INTRODUCTION

Amorphous mineral colloids are important in soils because their high reactivity affects the plant nutritional status, the water holding properties and the engineering behavior of soils.

The soils developed from volcanic ash contain predominantly amorphous mineral colloids. These soils are very important around the Pacific basin, particularly in Hawaii, where 50% of its agricultural soils are of volcanic ash origin. In soils not developed from volcanic ash, the main secondary minerals are crystalline. However, the small amounts of amorphous mineral colloids which these soils contain may still significantly affect their properties.

There are several hypotheses which account for the reactivity of the colloids. They are summarized as follows:

1. The high surface area of the colloids
2. The highly disordered internal structure
3. The intensive isomorphous substitution of Fe and Ti for Al, Al for Si in alumino-silicates, or Ti for Fe in amorphous iron
4. The coordination number of Al (either 4 or 6); the high activity of 4-coordinated Al in amorphous mineral colloids
5. The polymerization of aluminum hydroxide and its acid dissociation behavior

Although these hypotheses have been suggested by many investigators, they still remain controversial.

The objectives of this study were:

1. To investigate the morphology, structure, and the transformation of amorphous mineral colloids to crystallized minerals
2. To determine the range of chemical composition
3. To study the surface character and its relationship to the chemical properties of the amorphous mineral colloids

These studies may directly or indirectly clarify the hypotheses speculated.

LITERATURE REVIEW

Highly reactive amorphous minerals greatly affect the properties of most volcanic ash soils. In order to understand the reactions occurring at the surfaces of the soil particles, the physico-chemical properties of these minerals must be studied.

In Japan and New Zealand where many of the agricultural land soils come from volcanic ash, much attention has been paid to amorphous minerals, particularly allophane. However, many of the studies concerning amorphous mineral colloids still remain controversial. Some of the physico-chemical and mineralogical studies in the literature are reviewed here.

Definition and Constitution of Allophane

Amorphous minerals in soils include allophane, palagonite, and the hydrous oxides of alumina, silica and iron. Palagonite occurs in very slightly weathered soils, the hydrous oxides only in soils weathered under tropical conditions. Allophane, according to Fieldes (1955), is the name given to all amorphous colloidal minerals. Fieldes classified allophane into allophane A, allophane B and allophane AB. Allophane A is the cross-linked allophane in which the silica and alumina are chemically bonded through oxygen. Allophane B is a physical mixture of discrete silicas and alumina. Allophane AB is a mixture of allophane A and allophane B.

Egawa (1964), however, questioned the existence of allophane B. He said that the silica, alumina, and hydrated iron oxides may occur structurally combined with allophane (allophane A) and constitute a part of allophane itself. Thus allophane would not be a mere mixture of silica and hydrated sesquioxides, but a structurally or chemically combined body of these minerals.

Finally, Swindale (1964) proposed that the term allophane should be restricted to minerals with a SiO_2/Al_2O_3 ratio between one and three.

All of these definitions agree that allophane has a high reactivity, amorphous to x-ray, and has a large active surface area, but further study is needed to clarify the term "allophane".

Formation of Allophane

Swindale and Sherman (1964) pointed out that the genesis of soils derived from volcanic ash is closely allied to the weathering of volcanic glass, especially where the weathering intensity is high. They also stated that in early stages, volcanic glass weathers to palagonite, which is probably an amorphous alumino-silicate. This amorphous mineral alters predominantly to allophane in temperate and subtropical climates and to oxides in humid tropical climates. These minerals are usually associated with kaolin minerals produced in the weathering of the crystalline components of ash.

The manner in which allophane colloids are formed is still not generally agreed upon. Birrell (1964) proposed that volcanic ash is weathered first to discrete units of silica-gel and alumina-gel, and then through random cross-linking, develops into allophane. He constructed the following scheme for the formation of allophane:

silica + alumina (discrete) ⟶ silica + alumina (discrete) + (Allophane B)

silica-alumina ⟶ silica-alumina ⟶ metahalloysite
(Allophane AB) (Allophane A)

Ohmasa (1964) shares this idea of the formation of allophane and halloysite. On the other hand, Egawa (1964a) suggested that silicic acid and aluminum hydroxide, which originate from volcanic ash, co-precipitate isoelectrically with desilication and leaching of bases to form allophane.

Swindale (1964) questioned both of these mechanisms, stating that the formation of allophane is related to the stability of tetrahedrally-coordinated silicon. He proposed that the genesis of allophane is simpler than has so far been suggested, consisting first, the hydration of volcanic glass, then the loss or diffusion of bases and silica, and finally, the break-up of the glass fragments into smaller, highly hydrated units. Although the process of allophane formation is not definitely known, it is generally agreed that allophane precedes halloysite in the weathering sequence of volcanic ash.

Physico-chemical Properties of Allophane

Microscopic Morphology

Allophane does not have a definite micromorphology because its shape varies from sample to sample. However, some common micromorphological characteristics can be found. Aomine and Yoshinaga (1955) observed some irregularly shaped particles and aggregates of these particles which they called allophane. They also found some very fine, long, hair-like fibrous particles. In 1962 they observed some thread-like material of relatively uniform size, which they called "Imogolite". They consider this the intermediate mineral between allophane and well crystallized minerals.

Fieldes (1955) investigated the micromorphology of allophane in relation to weathering and formation of clay minerals. He noted that allophane B consists of very fine irregularly-shaped particles and that particle size increases as weathering increases. Curled plates and tubes of halloysite appear as weathering proceeds.

Egawa (1964) mentioned that electron micrographs generally show sponge-like nodular aggregates of small particles without definite regular shape. The shapes gradually change with aging and crystallization of allophane to halloysite.

Information about how the less crystallized, fibrous material develops into more crystallized particles and finally into tubular

halloysite is unavailable. It should be very interesting to study the mechanism by which the fibrous material is transformed into plate-like and then tube-like material.

Structure

Crystallinity

Allophane is x-ray amorphous, but as Egawa (1964) pointed out, its x-ray amorphism does not mean that the atomic arrangement of allophane is irregular or has no periodicity, such as regular tetrahedral and octahedral coordination. Fieldes et al. (1956) have pointed out that the x-ray method is suited to the study of materials with reasonably well-ordered structures and whose particle sizes are not much less than 0.1 micron in diameter. Therefore the structure and crystallinity of allophane cannot be studied by x-ray methods.

Yoshinaga and Aomine (1962) reported that x-ray diffraction patterns for randomly oriented allophane had two diffraction bands around 3.34 Å and 2.25 Å. White (1953) reported similar diffraction patterns for Indiana allophane. Some broad, very weak bands around 12-16 Å were noticed for oriented allophane by Aomine and Yoshinaga (1955). They suggested that small amounts of 2:1 minerals or mixed layer minerals were present.

Differential thermal analysis (DTA) patterns for allophane are important in identifying allophane. Fieldes (1955) reported that DTA patterns for allophane A have a single broad

endothermic peak with a maximum between 150-200°C., and an exothermic peak around 900°C. Samples containing discrete phases of silica and alumina (allophane B) show two discrete endothermic peaks in the region 100 to 200°C. and usually do not have the exothermic peak around 900°C. However, Egawa (1964) reported that some samples which seemed to possess the nature of allophane B do not show the two discrete endothermic peaks at 100-200°C. as Fieldes claimed.

Another endothermic reaction has been observed. Mitchell and Farmer (1962), Fieldes (1955), and Yoshinaga and Aomine (1962) have mentioned that the loss of structural hydroxyl groups is gradual. Consequently, there are no distinct endothermic peaks corresponding to those shown by most crystalline clay minerals in the 500° to 700°C. range. However, Sudo (1953) reported that piperidine-treated allophane shows characteristic exothermic peaks at 470°C. and at 310°C.

The infrared absorption technique has been used frequently for studying clay minerals. Some work on allophane has been reported. Fieldes (1955) stated that allophane A shows a broad band between 12.5μ to 8.17μ without any evidence of sharp peaks of crystalline silica or broad peaks of amorphous silica near 12.5μ. Allophane B shows a broad peak at 12.5μ in addition to the broad band in the 11.8 to 8.17μ region. Yoshinaga and Aomine (1962) got similar infrared patterns for allophane A.

From Egawa (1964) and Beutelspacher and van der Marel (1961), it is noticed that a slight shift of the 9.80μ peak toward longer wavelengths occurs with decreasing weathering intensities from kaolin to allophane, which may indicate the coordination status of aluminum and silicon in the minerals.

Coordination State

The coordination of aluminum ion in allophane is closely related to the structure, physico-chemical properties, and formation of allophane. Aluminum ion is found in both four and six coordination states in mineral structures because of its small ionic diameter, 0.5 Å. (Milliken et al., 1950). Jackson (1963) has pointed out that in igneous rocks formed at high temperatures, aluminum is largely in the four coordination. As pedogeochemical weathering proceeds, aluminum attains the six coordination. Swindale (1964) has mentioned that the reactivity of allophane is probably due to the acid character given it by the four-coordinated aluminum. He also pointed out that most allophanes have SiO_2/Al_2O_3 ratios below two, a value too low to stabilize four-coordinated aluminum throughout the structure as proposed by Milliken (1950). Thus Swindale suggested that the four-coordination state occurs only in zones within the crystal, the remaining alumina being six-coordinated.

Egawa (1964b) determined the coordination of aluminum by x-ray fluorescence. He got a statistical average coordination

number of five, indicating that aluminum ion is in both four and six coordination states.

Infrared spectroscopy has also been used for determining the coordination number in amorphous silicoaluminas by Leonard, Suzuki, Fripiat, and De Kimpe (1964), and by De Kimpe, Gastuche and Brindley (1964). The Si-O stretching bands in 9-10 μ region was used as an index, and the percentage of four-coordinated aluminum can possibly be determined by the shift of this absorption maximum.

This shift may be due to two factors: Differences in the silica-alumina ratio and the degree of substitution of Al for Si. According to Mitchell and Farmer (1962), it is to be expected that the maximum absorption of the Si-O band in allophane will shift to shorter wavelengths with increasing degrees of polymerization of the silica tetrahedral in the structure. For example, with an increased silica to alumina ratio, the Si-O band may shift from between 10 and 11 μ, for isolated tetrahedral, to 9 μ for highly polymerized tetrahedra as in silica gel. The substitution of Al for Si in the tetrahedra network should cause a displacement to a longer wavelength for any given degree of polymerization (Mitchell and Farmer, 1962). These speculations should be checked experimentally before they can be used for quantitative analysis of Al coordination. If the first factor is kept constant by choosing minerals with the same silica-alumina ratio, we probably

can determine the percent of four coordinated Al from the shift of Si-O band.

Surface Character

It is generally agreed that allophane has a large specific surface area and strong reactivity, and the latter is closely related to the surface charge behavior. Allophane has both positive and negative charge and acts as an amphoteroid, with a relatively high isoelectric point. These characteristics are somewhat different from those of the crystalline clay minerals.

Origin of Charges

Grim (1953) and Wiklander (1964) have stated that clays possess an amphoteric character and are able to bind both cations and anions. In general, they carry a net negative charge. The negative charge arises essentially in three ways: (1) from isomorphous ion substitution, (2) from ionization of hydroxyl groups attached to silicon and alumina, and (3) from defects in the structure. Positive charge may originate from hydrous oxides of iron and aluminum which react as bases by accepting protons from the environment or from defects in the structure.

Behavior of Charges

Russell (1961) has shown a general change of net charge with respect to pH. As the pH increases from 2 to 11, the net charge increases gradually. Schofield (1949) reported that for clay the change in net charge from pH 2.5 to 6 is due to the

decrease in the number of positive charges, little or none being due to increase in the number of negative charges. From pH 6 to 7.5, on the other hand, the rise in negative charge is due to an increase in the number of negative charges.

Sumner (1962) has demonstrated that iron oxides develop negative charges, under alkaline conditions, and contribute significantly to the pH-dependent negative charge in soils. He depicted the change in charge, which may also be true for aluminum hydroxides, as follows:

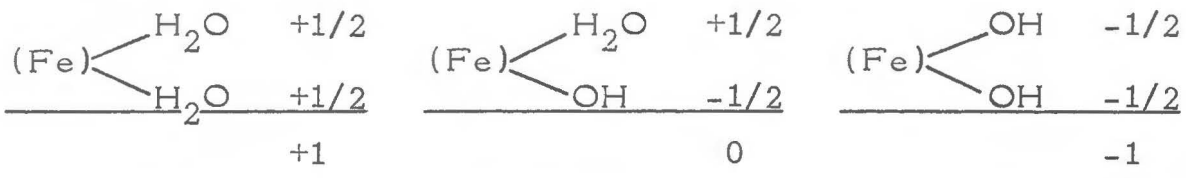

Acid Isoelectric Point Alkaline

It is interesting that Schofield (1949) showed the permanent negative charges between pH 2.5 and 5 as probably due to isomorphous ion substitution.

Cation Exchange Capacity and Base Saturation

The cation exchange capacity (CEC) of allophane is generally high and extremely pH-dependent. It also depends on the concentration and the cations in the leaching solution and the water content of allophane as shown by Birrell and Gradwell (1956). Thus the CEC values fluctuate due to slight changes in experimental conditions and reproducibility is difficult.

The CEC of allophanic clay was 23.3 to 57.3 me./100 g and 54 me./100 g, as determined by Aomine and Yoshinaga (1955) and by Birrell and Fieldes (1952), respectively.

Birrell (1964) mentioned that base saturation of allophane could be very low although the pH values remain comparatively high. Swindale (1964) questioned the reliability of base saturation determinations. He stated that amorphous mineral colloids have pH-dependent charges and the apparent base saturation determined in the laboratory at pH 7 may be much lower than the true base saturation of the soil under field conditions with a pH lower than 7. Further study is necessary in order to provide a standard method of determining CEC for allophane-containing soils.

MATERIALS AND METHODS

Soil Samples

The following samples of Hawaiian and Japanese soils were selected for this study because they are known to be rich in allophane and have varied silica-alumina ratios.

Table I. Source and Description of Soil Samples

Great Soil Group	Soil Series	Location	Depth	SiO_2/Al_2O_3 of the Clay
	Choyo	Japan	30-75"	1.12
Hydrol Humic Latosol	Kealakekua	Hawaii	23-36"	0.96
Latosolic Brown Forest	Kaipoioi	Hawaii	48-61"	1.01
Hydrol Humic Latosol	Akaka	Hawaii	50-74"	0.99
Reddish Brown	Waikaloa	Hawaii	28-31"	2.09

Choyo, a Japanese soil, has been described and studied by Aomine and Yoshinaga (1955) and Yoshinaga and Aomine (1962). The SiO_2/Al_2O_3 of this soil was taken from their studies. The Kaipoioi and Kealakekua series have been described and studied by Tenma (1965). The Akaka and Waikaloa series have been described by Kanehiro (1965) and Houng (1964), respectively. The SiO_2/Al_2O_3 ratios of the four Hawaiian soils were taken from Tenma's study.

Clay Separation

The method for the separation of allophane from soil samples proposed by Yoshinaga and Aomine (1962) has been followed in this study. The flow sheet of the method is presented in Fig. 1.

Moist soil was treated with H_2O_2 to remove organic matter, deferrated with citrate-dithionite, then boiled in 2% Na_2CO_3 solution for 5 minutes to remove free silica and alumina (Jackson, 1956).

The treated soil was dispersed in NaOH (pH 10.5) and separated at 2 microns. After the clay was dispersed and separated exhaustively in an alkaline medium, the still undispersed portion was dispersed in dilute HCl (pH 4.0) and separated at 2 microns. The alkaline-separated clay of less than 2 microns was further separated at 0.1 micron using the Sharples super-centrifuge as described by Jackson (1956). The alkaline-separated, less than 0.1 micron fraction is considered to be allophane by Yoshinaga and Aomine (1962).

The alkaline- and acid-separated fractions were flocculated by changing the pH. Whenever necessary, NaCl was also added to promote flocculation. The flocculated clays were saturated with sodium by using NaCl and NaOAc. Excess salts were washed out with water, water-methanol, and then a methanol-acetone mixture to prevent premature dispersion. Finally, the washed clays were stored with water containing a little methanol

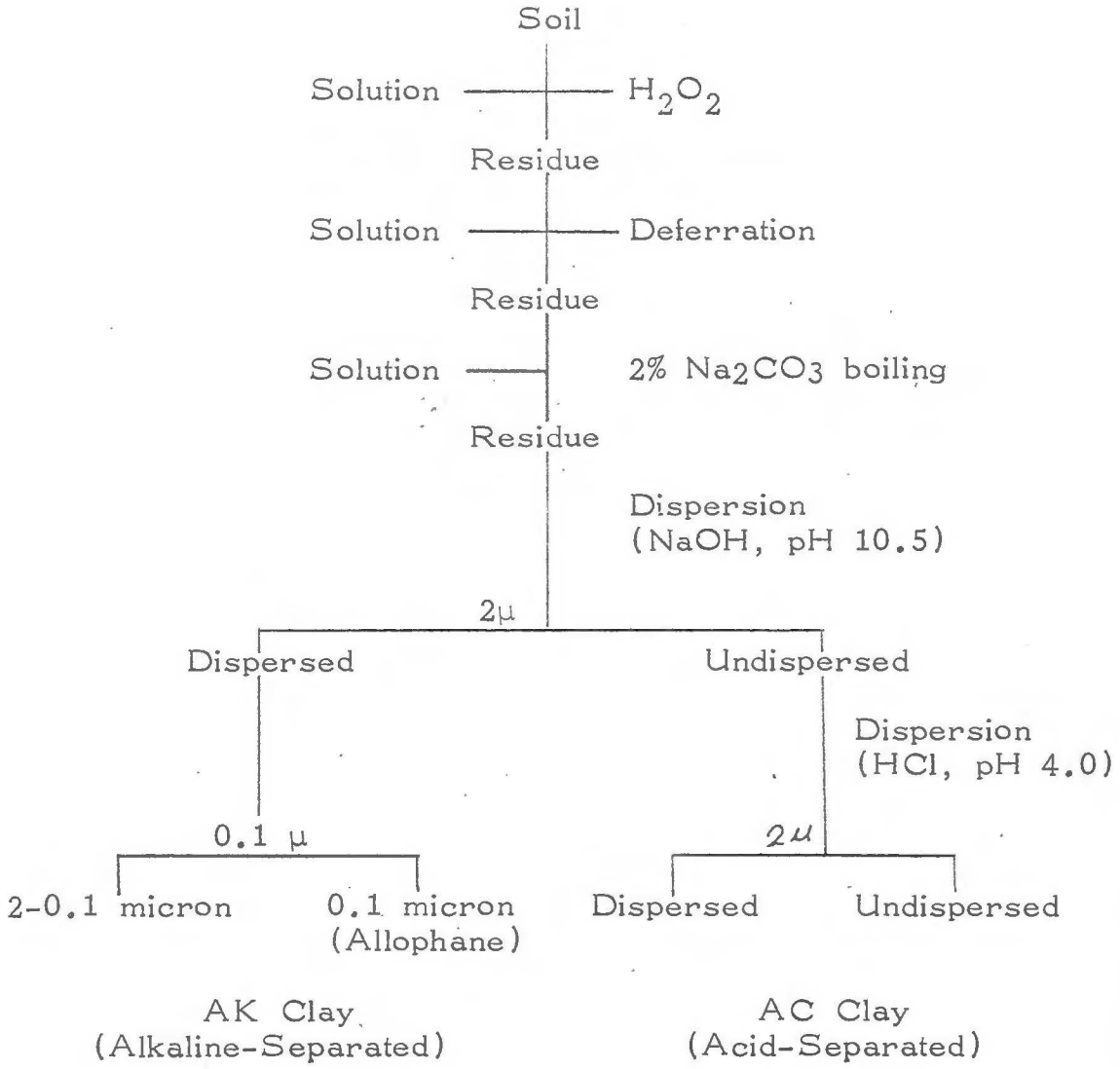

Fig. 1. Flow Sheet for Allophane Separation

in jars.

X-ray Examination

The amorphous clays used in the present study curled up when they dried on the x-ray slides. Therefore caution was taken to prevent this by putting one drop of 50% glycerine on the slide before pipetting 1 ml. of approximately 1% clay suspension onto it. Diffraction patterns of the oriented clays were obtained by using a Philip-Norelco x-ray diffractometer.

Differential Thermal Analysis (DTA)

Air-dried clay was ground to pass a 100 mesh sieve. The sample was then kept in a vacuum desiccator containing saturated $Mg(NO_3)_2$ solution to obtain a relative humidity at about 57% for 72 hours.

0.100 gm. of clay was mixed with 0.130 gm. of calcined alumina, which is also the reference material. Differential thermal analysis was run on Stone's automatic DTA machine at the rate of 10°C. per minute between 25 to 1050°C.

Chemical Analysis

Allophane is mainly composed of silica, alumina and water. It was speculated at the beginning of this study that the relative amounts of silica, alumina, and the bound and adsorbed water may be related to the physico-chemical properties and structure.

Loss on Ignition

0.2 gm. of oven-dried clay was placed in a platinum

crucible and gradually ignited to 800°C. for 1 hour. The loss of weight was assigned to structurally bound water.

Fusion of Clay

Shapiro and Brannock's (1962) method was used. 0.1500 gm. of ignited clay was fused with NaOH in a nickel crucible. After fusion the cake was disintegrated in water in the crucible, and the solution made acidic with HCl, and then brought to volume for silica and alumina determinations.

Silica Determination

Silica tends to polymerize in acid conditions. Therefore the amount of silica was determined immediately after the solution was prepared from the fused material. The molybdenum blue method of Bunting (1944) was used, and the percent transmission was determined at the wavelength of 640 mμ on a Beckman DU spectrophotometer.

Alumina Determination

Alumina was determined volumetrically by the EDTA titration method of Gorcey de Longuyen (1958) as used by Swindale (1961). Excess amounts of EDTA were added to the solutions containing Al. The EDTA forms complex ions with Al as well with other metal ions. The excess free EDTA was titrated with $Zn(OAc)_2$. NaF was added and the solution boiled. The amount of EDTA released during boiling in NaF is equivalent to the amount of Al present. The released EDTA is titrated

with dilute $Zn(OAc)_2$.

Electron Microscopy

Dispersion mounts on collodion-covered, 400-mesh, 1/8-inch grids were prepared to study the size and morphology of the clay samples. The details of sample preparation and examination are described in the following sections.

Preparation of Grids

In order to cover a thin film of collodion on the grids, the procedure proposed by Rich and Kunze (1964) was used.

a. Three drops of 2% collodion amyl acetate solution were put on a one-liter beaker filled with distilled water. A watch glass was placed over the beaker to retard evaporation.

b. After about three minutes, the collodion dried and formed a film on the water surface.

c. The grids were placed with the smooth side directly on the film. For convenience, nine grids were placed in three rows at one time.

d. A clean glass slide was lowered with its vertical edge onto the film surface in such a manner that the film and grids adhered to one side of the slide. When the slide was removed from water, the film fell flat onto the slide with the grids lying under the film.

e. The grids dried on the slide, being held quite firmly by

the film. At this point, the grids were ready to be mounted with the sample suspension. It is best to leave the grids on the slide while mounting the sample.

Dispersion of Clay

One ml. of approximately 1 percent clay suspension was diluted 1000 times with three repeated dilutions of 1 to 10 in a 15 ml. test tube. The final diluted suspension was shaken for 15 minutes on a shaker to promote dispersion. One drop of the suspension was placed with a medicine dropper on the film-covered grid and allowed to dry.

Shadowing and Carbon Coating

A shadowing technique was used to increase contrast, revealing surface configurations and providing a measure of thickness. Uranium metal was used and shadowed at an angle of $\tan \theta = 1/3$.

Both shadowed and unshadowed samples were sprayed with carbon vapor to strengthen the specimen so that it could withstand the electron beam while being observed under the microscope.

Electron Microscopic Examination and Photography

Each specimen was observed under a Norelco Electron Microscope, Type EM 75, at 40 to 50 positions. Three to five representative views were photographed at a magnification of 14600 X.

Infrared Absorption Spectroscopy

A KBr pellet of dry sample was prepared for infrared absorption analysis on a Beckman IR-9 infrared spectrophotometer. The detailed procedure is as follows:

Pellet Making

Approximately 250 mg. of oven-dried, IR-grade KBr was weighed into a small agate mortar. Two mg. of clay equilibrated at 57% relative humidity was weighed out and mixed thoroughly with the KBr. One-half of the mixture was placed in a pressure disc on a hydraulic press. The vacuum was connected to the disc, then pressure was gradually brought up to about 10 tons per in^2 within 3 minutes and maintained for another 3 minutes.

According to Rich and Kunze (1964), the pellet should be fairly clear without noticeable spots of clay. Pellets were kept in a vacuum desiccator when not used immediately.

Infrared Spectroscopy

The Beckman IR-9 spectrophotometer is a highly effecient instrument with high resolution and a wide range of scanning. A KBr prism covers the scanning range of 2.5 to 25 μ and a CeI prism for the 15 to 50 μ range. The slits can be automatically controlled, and use of the double beam will cancel out the absorption caused by materials other than the sample in the pellet.

In this study, the scanning covered the wavelength range of 2.5 to 25 μ equivalent to the wave number range of 4000 to

400 cm^{-1}. The absorption patterns were obtained at a gain of 6% and at a scanning speed of 80 cm^{-1}/min.

Several reference minerals were used to obtain reference IR patterns.

Surface Area Determination

Greenland and Quirk's (1964) method was used for surface area determination. In this method, cetyl pyridinium bromide (CPB) solution was adsorbed by the clay, and the surface area measured from the amount of CPB adsorbed.

Procedure

a. A clay suspension containing 0.1000 to 0.1500 gm. of clay was pipetted into a 100 ml. centrifuge tube. If the sample was air-dried, then it was weighed out.

b. Forty ml. of 0.3% (or other suitable concentration) CPB was added to the centrifuge tube.

c. The mixture was shaken for 18 hours.

d. The mixture was then centrifuged at 2000 rpm. for 10 to 20 minutes. (To avoid evaporation during centrifugation, the tubes were kept covered.)

e. A 4 to 10 ml. aliquot of the supernatant was put in a 100 ml. volumetric flask and brought up to volume. (At this stage, the solution was still cloudy at times.)

f. Ten ml. of the solution was put in a 50 ml. centrifuge tube and 1 N $CaCl_2$ was added to flocculate the clay.

g. The mixture was centrifuged at 2000 rpm. for 10 minutes. (This time the supernatant was clear.)

h. The supernatant was decanted into a 100 ml. volumetric flask and made up to volume.

i. Transmittance was measured in the ultraviolet region at 259 mμ on a Beckman DU spectrophotometer using a hydrogen lamp and a blue phototube.

Calculation of Surface Area

From Greenland and Quirk (1962), one CPB ion covers 27 A^2 of area. Therefore one milli-equivalence of CPB covers 162 m^2 of area. The formula for calculating surface area from the amount of CPB adsorbed is:

$$S = a \times 162$$

S = Specific surface area in m^2/g

a = Amount of CPB adsorbed in me./g

Cation Exchange Capacity and Its pH Dependency

The negative charge behavior was studied by determining the cation exchange capacity (CEC) at different pH levels. The CEC was determined by a method developed by Pratt (1961) at pH levels 4.0, 5.5, 7.0 and 8.5.

0.5 gm. of clay which was not pre-dried was used for this determination. Because the clay tended to disperse in methanol, a water-acetone mixture was used for washing away excess salts. Since $BaCl_2$ is not soluble in pure acetone, care was taken to

wash the sample with 50% acetone, then to increase the concentration of acetone gradually to avoid dispersion. The concentration of acetone should not be higher than 95% for the final washing.

The amount of Ba ion in the sample was determined by flame photometry on a Beckman DU photometer at a wavelength of 553.6 mμ.

RESULTS AND DISCUSSION

X-ray Diffraction Analysis

The diffraction patterns for the oriented clays show very significant differences between the fine clay (less than 0.1 micron) and coarse clay (2 to 0.1 micron) for each sample. They are shown in Fig. 2 and Fig. 3.

Generally, the fine clay appears x-ray amorphous with the exception of Waikaloa, although there is a recognizable diffraction band around 17 to 10 Å. This band increases in intensity in the following order:

Choyo----Kealakekua----Kaipoioi----Akaka

This band indicates the presence of weakly formed 2:1 minerals. For Waikaloa fine clay, a broad but clear peak at 11 Å was identified as hydrated halloysite.

For the coarse clay, Choyo and Waikaloa show the least degree of crystallinity. Choyo shows a band in the 17 to 12 Å region, which is similar to the fine clay fraction. Waikaloa shows a very weak hydrated halloysite peak at 11 Å. Kealakekua, Kaipoioi, and Akaka form a sequence with increasing intensity of mica, kaolinite, and gibbsite peaks from Kealakekua to Akaka. Quartz was also identified in Akaka.

The crystallinity for the fine and coarse clay fractions can be summarized as follows:

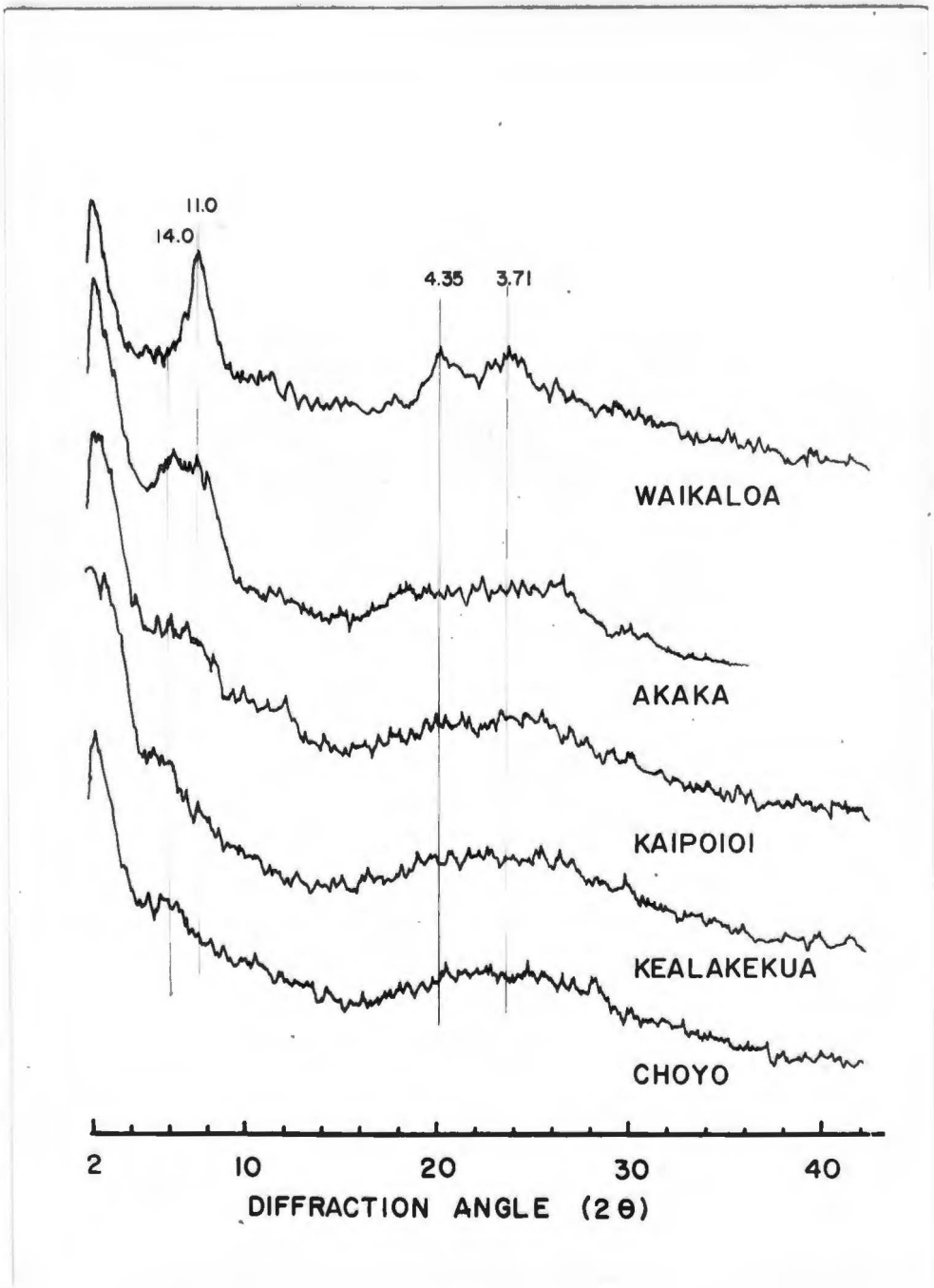

Fig. 2. X-ray Diffraction Patterns of the Fine Clay Fractions

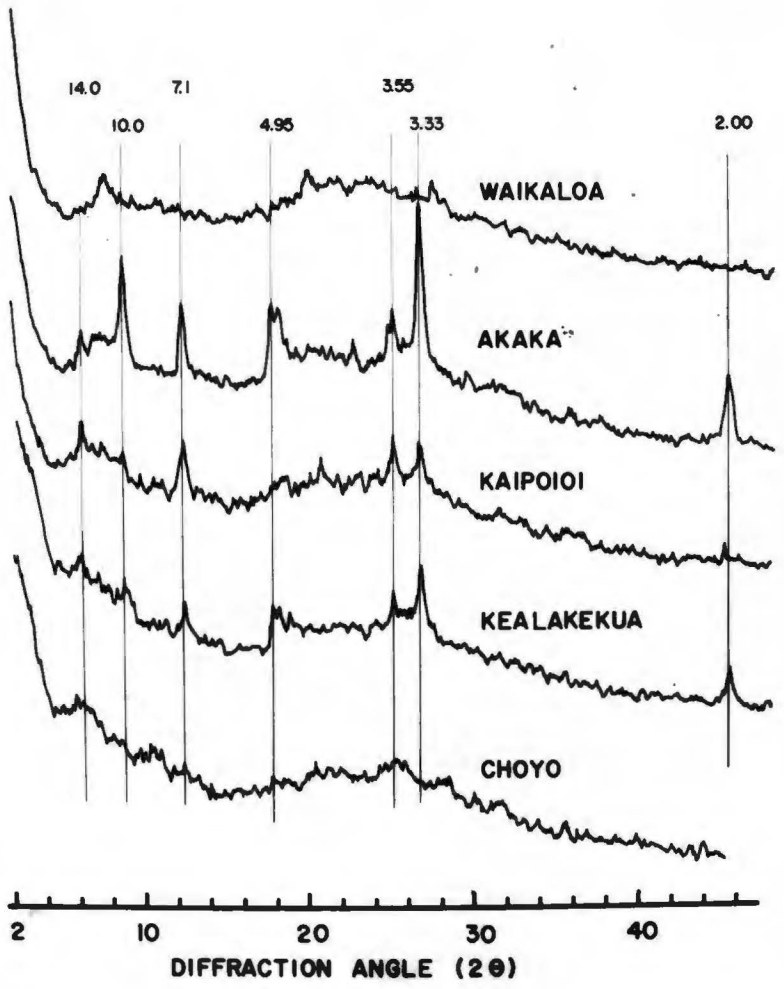

Fig. 3. X-ray Diffraction Patterns of the Coarse Clay Fraction

Fine clay fraction		Coarse clay fraction
	Increasing Crystallinity	
Choyo		Choyo
Kealakekua		Waikaloa
Kaipoioi		Kealakekua
Akaka		Kaipoioi
Waikaloa		Akaka

Further discussions on crystallinity will be given in other sections.

Differential Thermal Analysis

Differential thermal analysis (DTA) patterns of the fine and coarse clay fractions are shown in Fig. 4 and Fig. 5. The general features of the DTA patterns for fine clays are: (1) a strong endothermic peak with the maxima between 100° and 150°C. and (2) an exothermic peak at about 850° to 950°C. These characters are comparable to those reported by Fieldes (1955), Yoshinaga and Aomine (1962) and Egawa (1964) for allophane. The exothermic peaks occurring in the 400° to 700°C. region are attributed to organic matter by Fieldes (1955). In Kaipoioi, there are two high temperature exothermic peaks at 870° and 990°C. In Akaka, there is a peak at 880°C. and a very weak peak at 940°C. The reason for these two separate exothermic reactions may be attributed to montmorillonite or other expanding micas. Waikaloa shows an endothermic peak at 490°C. which has been attributed to halloysite.

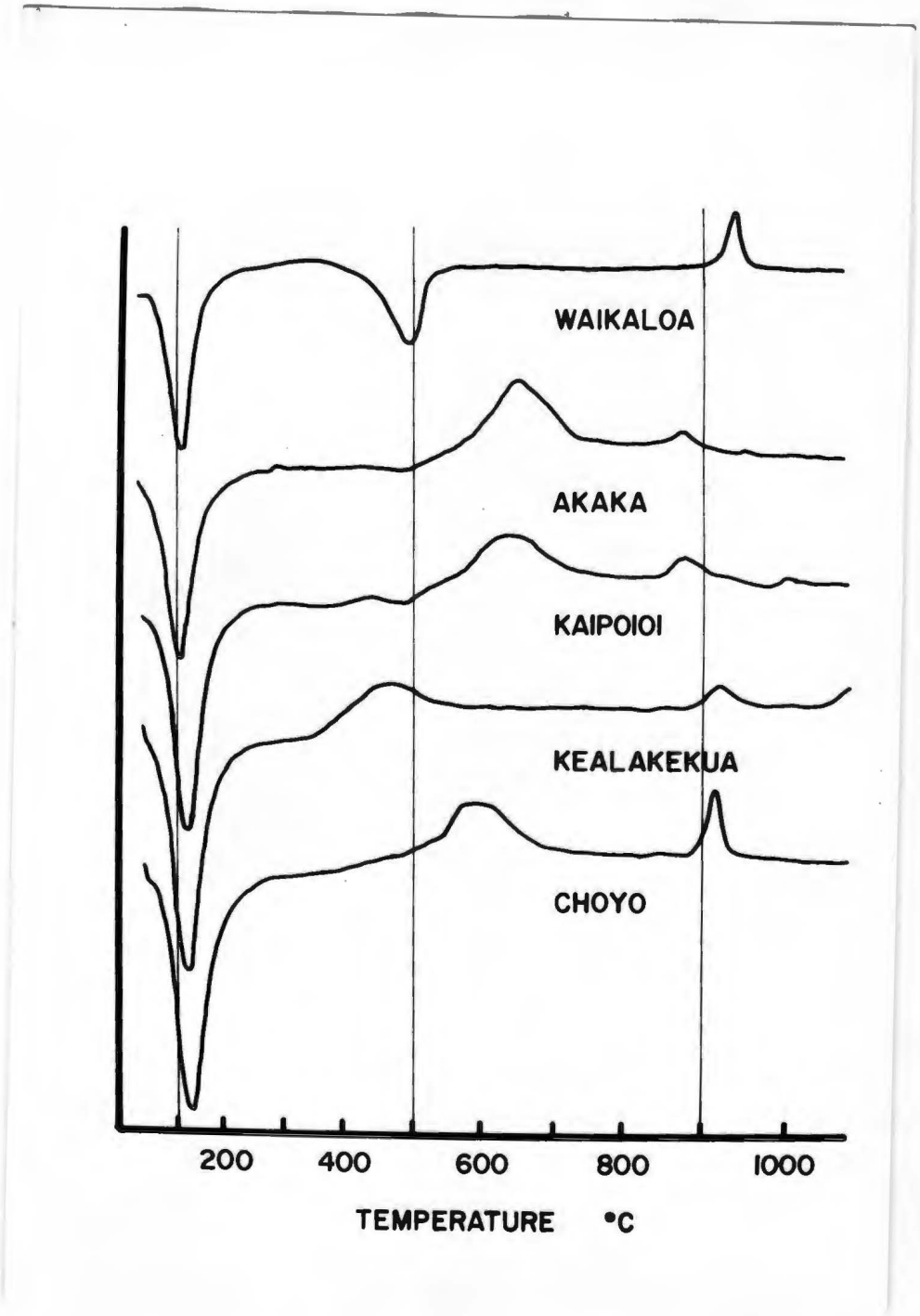

Fig. 4. DTA Patterns of the Fine Clay Fractions

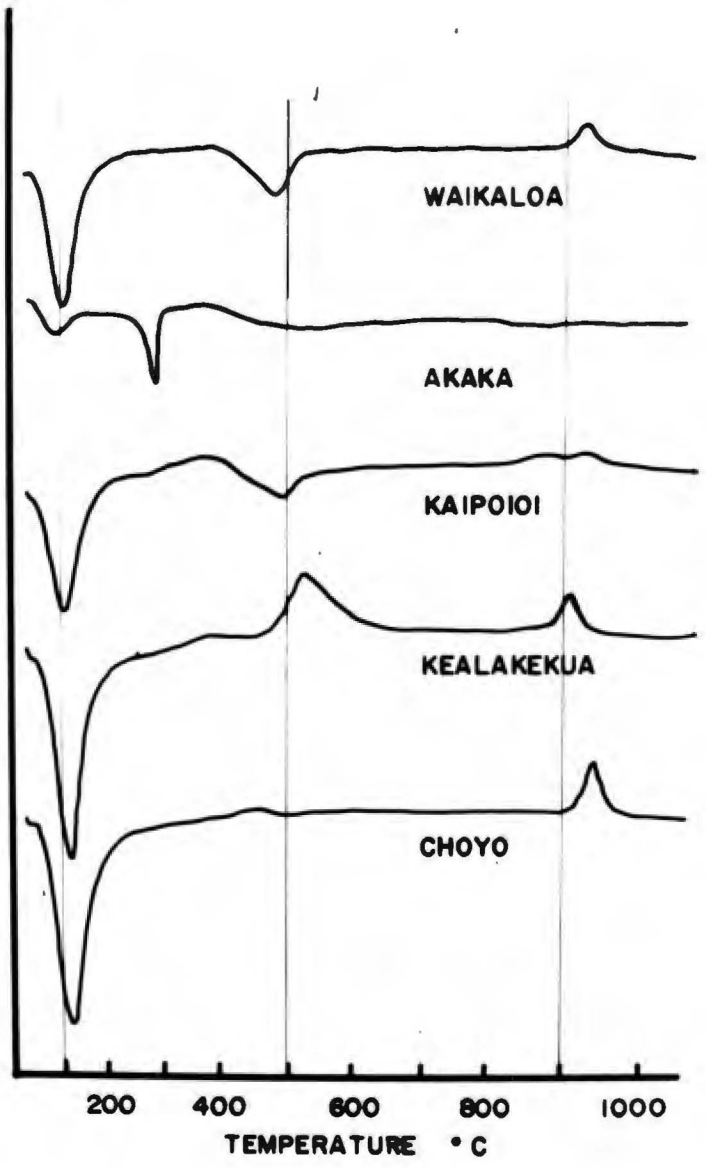

Fig. 5. DTA Patterns of the Coarse Clay Fractions

In addition to the features shown in the fine clay fraction, the DTA patterns for the coarse fractions show endothermic reaction between 250° and 500°C. Kaipoioi and Waikaloa show a weak endothermic peak at 495°C. due to halloysite. Akaka shows an endothermic peak at 295°C. due to gibbsite.

The area of the first endothermic peak is listed in Table II. The magnitude of the peak area is closely related to the crystallinity estimated from the x-ray data; the order of decreasing peak area being consistent with the order of increasing x-ray crystallinity. The adsorbed water which is released at lower temperatures is believed to be closely related to the surface character of allophane, and it may be possible to utilize peak area as an index for allophane.

The double endothermic maxima below 200°C. attributed to allophane B by Fieldes (1955) was not seen in this study.

Table II. First Endothermic Peak Area on DTA Patterns of the Five Clays (in^2)

Soils	Fine Clay	Coarse Clay
Choyo	2.03	1.95
Kealakekua	1.89	1.67
Kaipoioi	1.61	1.02
Akaka	1.45	0.16
Waikaloa	1.07	1.06

Elemental Analysis

The main purpose for the elemental analysis was to investigate the relative amounts of silica, alumina and the structural water, and their relationship to the structure and chemical properties of allophane.

From Table III and Fig. 6, it is noticed that the loss of ignition (LOI) decreases with an increasing SiO_2/Al_2O_3 ratio. Both LOI and SiO_2/Al_2O_3 are closely related to the degree of crystallinity.

Two questions are raised here:

1. Why is crystallinity related to SiO_2/Al_2O_3 ratio?
2. What role does the water play in the structure?

Apparently SiO_2 is essential for building up the structural framework. It acts as a stabilizing agent in the $SiO_2 \cdot Al_2O_3$ system. Milliken et al. (1950) have mentioned that the structural stability of Al in 4-coordination is highest when the weight percentage of Al_2O_3 is 30%. Beyond this, the 4-coordinated Al is unstable and tends instead to be 6-coordinated. In all the clays studied here, the Al_2O_3 content is greater than 30%. There is not enough SiO_2 to stabilize the structure of Al in the 4-coordinated state. Present knowledge is not in a position to answer the question why crystallinity is related to silica-alumina ratio.

Table III. Weight Percent of SiO_2, Al_2O_3, and Bound H_2O and Their Ratio

Soils	SiO_2 (%)	Al_2O_3 (%)	LOI (%)	$\frac{Al_2O_3}{Al_2O_3+SiO_2}$ (%)	$\frac{SiO_2}{Al_2O_3}$*
			Fine Clay		
Choyo	20.7	37.9	38.8	64.68	0.927
Kealakekua	21.6	38.9	36.5	64.30	0.943
Kaipoioi	23.3	33.1	33.5	58.69	1.194
Akaka	24.5	27.7	32.1	53.07	1.501
Waikaloa	29.5	32.8	24.8	52.65	1.527
			Coarse Clay		
Choyo	27.1	36.5	29.1	57.39	1.260
Kealakekua	24.8	31.2	27.7	55.71	1.349
Kaipoioi	27.2	28.7	22.5	51.34	1.609
Akaka	34.5	27.3	15.0	44.17	2.145
Waikaloa	34.4	30.1	19.2	46.67	1.940

*Molar Ratio

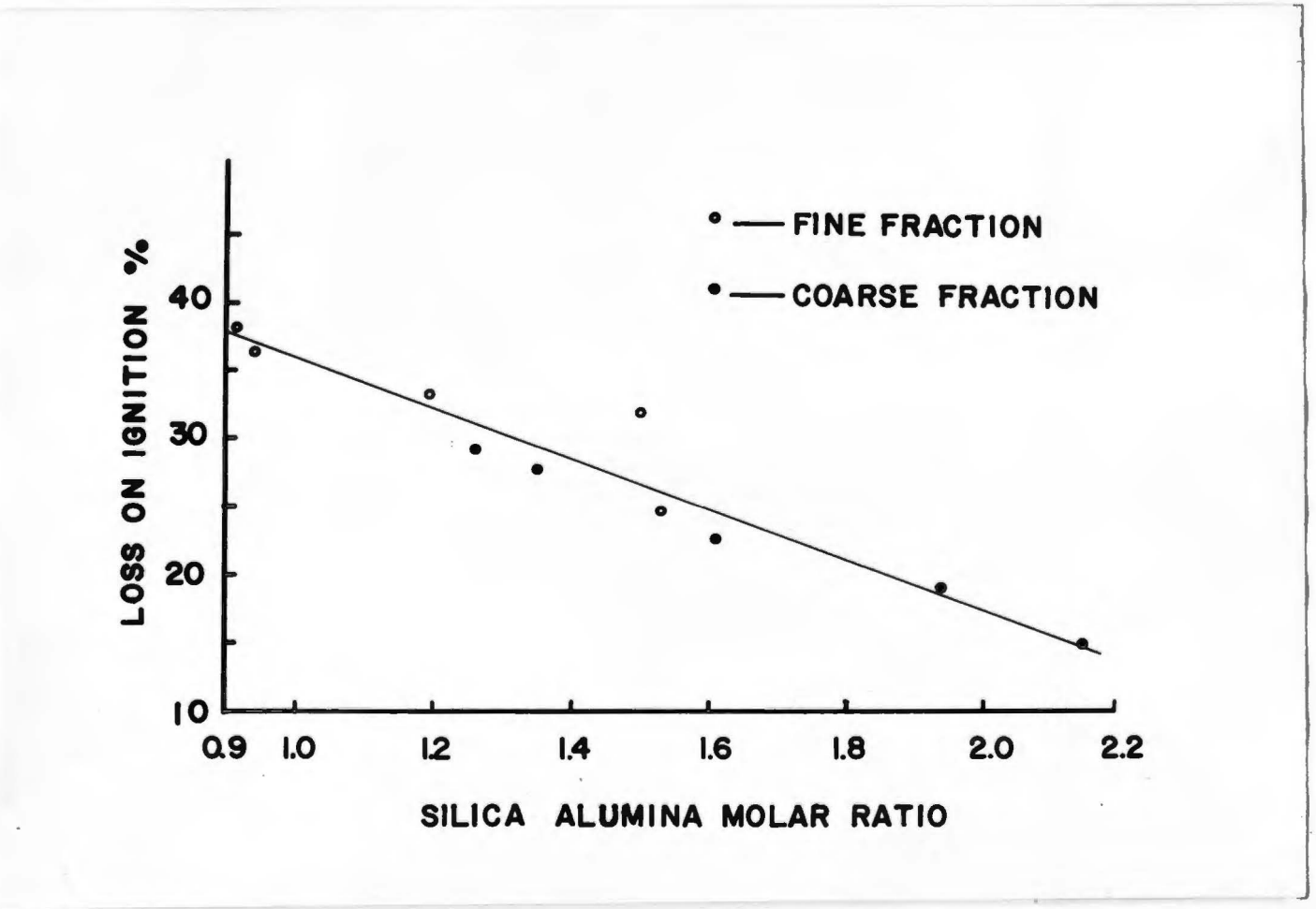

Fig. 6. Loss on Ignition Versus Silica-Alumina Ratio of the Five Clays

Water increases as SiO_2/Al_2O_3 decreases. This water obviously is related to Al. As the SiO_2/Al_2O_3 decreases, the 6-coordinated Al increases, and this increases the opportunity for OH to bond with Al^{VI}. The coordination state of Al will be discussed further in the section on infrared absorption spectroscopy.

The relationship between $Al_2O_3/(Al_2O_3+SiO_2)$ and ΔCEC will also be discussed in a later section.

Electron Microscopy

Electron micrographs show that the morphology of the fine clay fraction is significantly different from that of the coarse clay fraction. The size and shape of the particles appear to bear some relationship with the degree of crystallinity as determined by x-ray diffraction analysis.

Some common features of the fine clay are noticed in Figs. 7, 9, 11, 13, and 15 and are summarized as follows: (1) All the samples show microfibrils with diameters approximately 1/10 μ and lengths from 1/2 μ to several microns. They appear to be collections of small balls joined together. (2) There is a large amount of sponge-like material built up by many small balls. The sponge-like material, interconnected with the microfibrils, hold a great deal of empty holes with diameters varying from 1/10 to 1 μ. It is obvious that the fibrous and sponge-like structure will have a high specific surface area and will therefore render high reactivity to this material.

From micrographs of the coarse clay (Figs, 8, 10, 12, 14, and 16), it can be noted that the fibrous material and the sponge-like material decreases as the amount and size of the flakey material increases, i.e., allophane decreases as crystallinity increases.

As crystallinity increases, the morphology of the clay particles varies from irregular-shaped flakes (See Figs. 10 and 12) to pseudohexagonal flakes (See Fig. 14) or small tubular materials (See Fig. 15).

Some of the micrographs show very clear surface configuration. Fig. 18 of Akaka shows a large flake of 4-5 μ width with a Moiré pattern. The Moiré effect may be attributed to superimposed atomic lattices of slightly different atomic spacings and can indicate individual dislocations in a thin crystalline film (Haine and Cosslett, 1961). If the pattern in the Akaka flake is due to such an effect, these dislocations may very well render surface charges which can be an important factor in chemical reactivity. In Fig. 17, lower-right corner, several lines appear as the slip dislocation or edge defect. This will also render chemical reactivity to the clay.

The fine clay fraction of the Kealakekua was studied more critically with the Hitachi Electron Microscope, Type HU-11A, which has a greater magnification capacity than the Norelco Electron Microscope, Type EM 75. Figure 22 shows not only

fibrous and ball-like or sponge-like materials, but also some curled flakes and small tubes which appear to be halloysite. Such observation suggests that halloysite may be the initial transformation product of allophane.

Fig. 19 and Fig. 20 give clues as to how the allophane may be transformed to crystalline minerals. It is speculated that the fibrous material is closely joined together into a close network which gradually merges to form sponge-like flakes which finally become plate-like crystal. The supersaturated solution in voids of the network allows the structural transformation.

From the foregoing observation, it is believed that allophane is the fibrous material and the sponge-like material, both of which seem to be collections of small balls joined together in one, and three dimensions, respectively, with many holes between.

The "Imogolite" of Aomine and Miyauchi (1965) was not identified in this study, even in the sample Choyo, from which they obtained this material. Kealakekua (Fig. 21) shows some thicker threads connected with finer fibers, but it does not show any sign of a unique and different mineral distinct from allophane. The x-ray data also did not show any clear "Imogolite" pattern. Therefore, it is doubtful that "Imogolite" is separable from allophane.

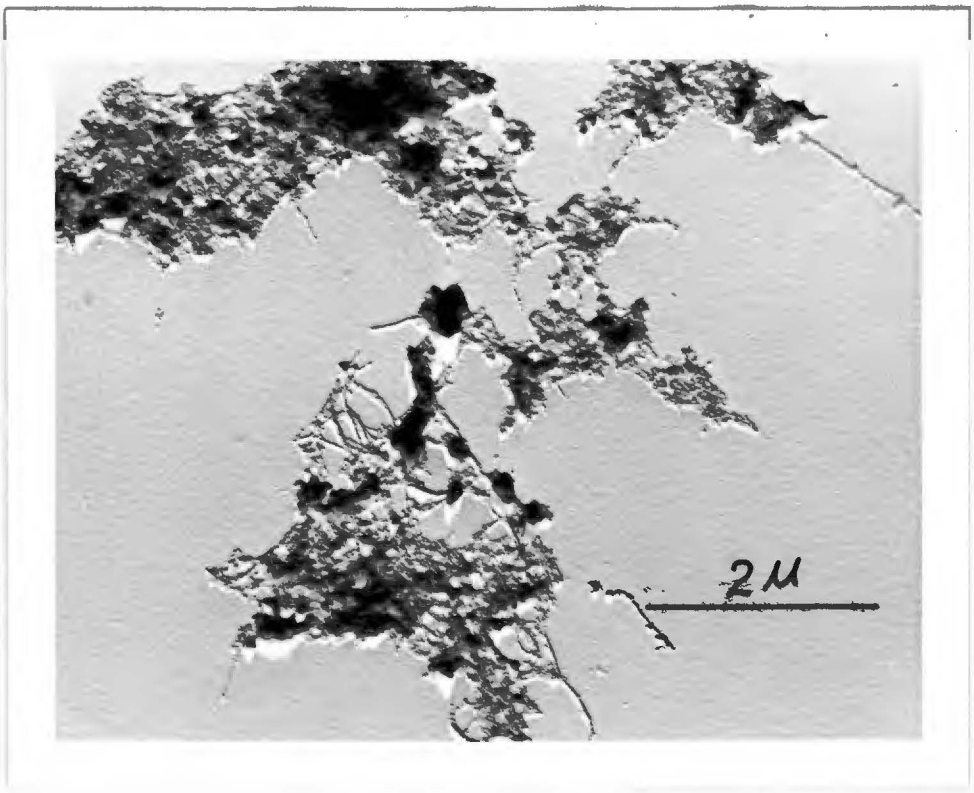

Fig. 7. Electron Micrograph of the Fine Clay Fraction of the Choyo Sample

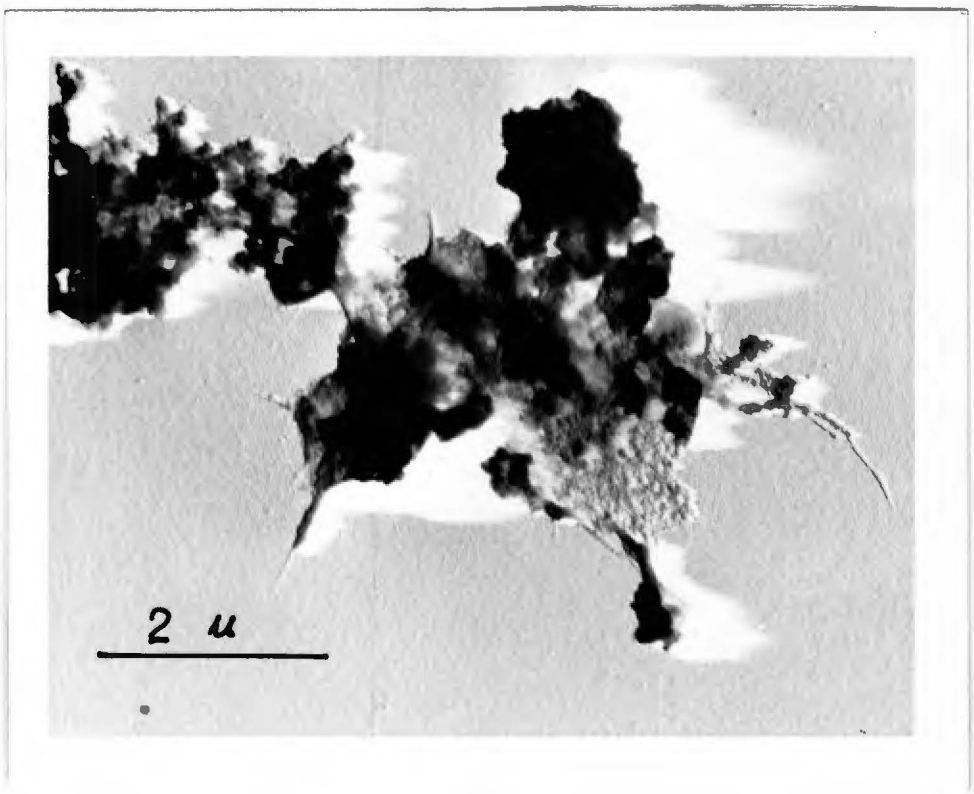

Fig. 8. Electron Micrograph of the
Coarse Clay Fraction of the Choyo Sample

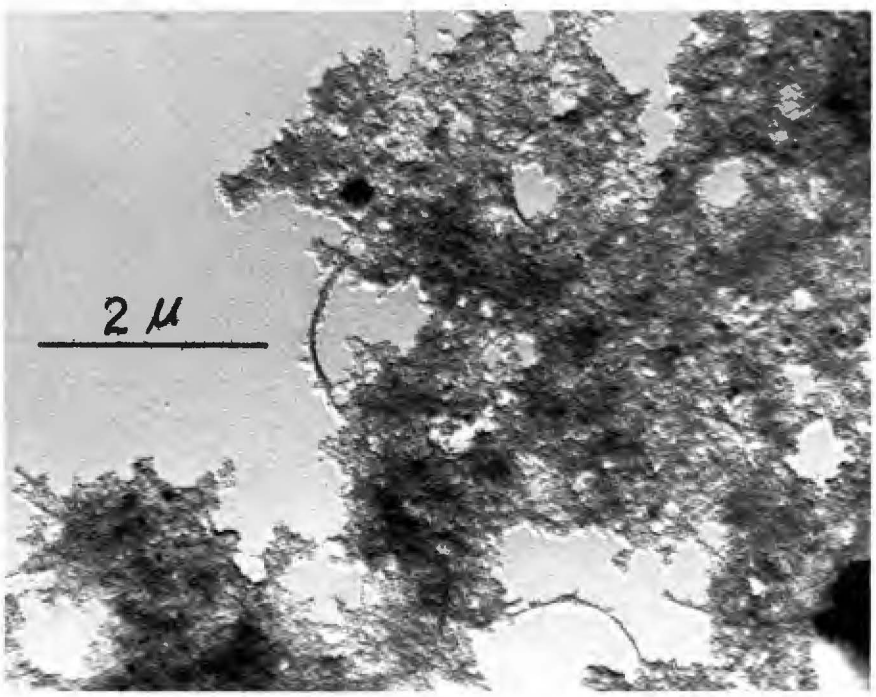

Fig. 9. Electron Micrograph of the Fine Clay Fraction of the Kealakekua Soil

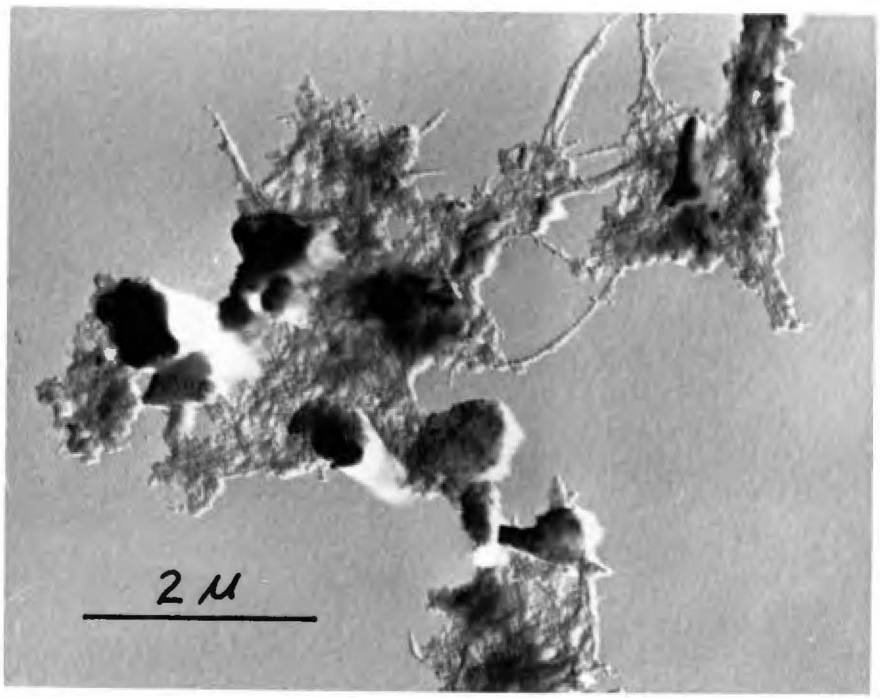

Fig. 10. Electron Micrograph of the Coarse Clay Fraction of the Kealakekua Soil

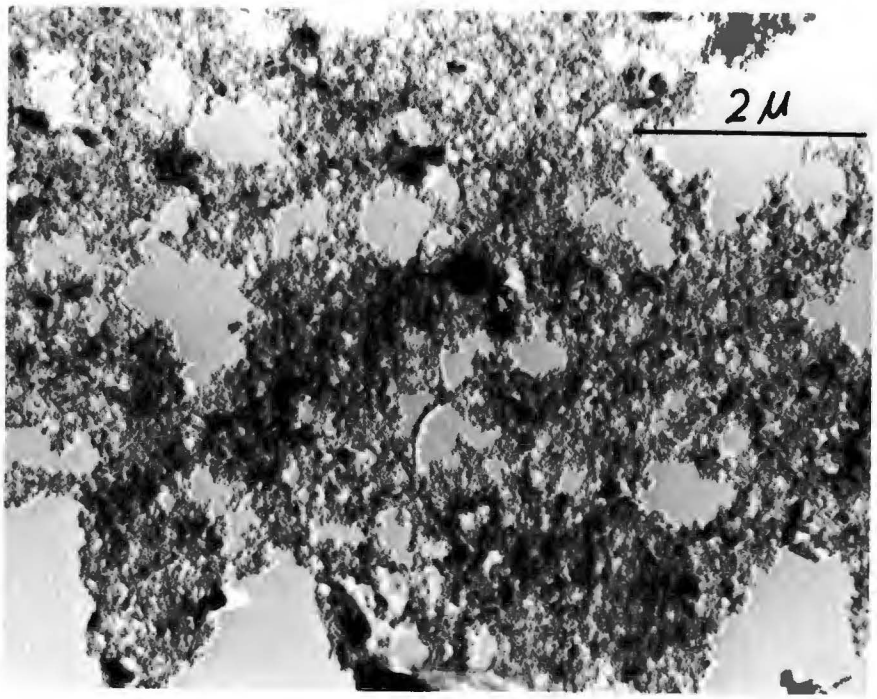

Fig. 11. Electron Micrograph of the Fine Clay Fraction of the Kaipoioi Soil

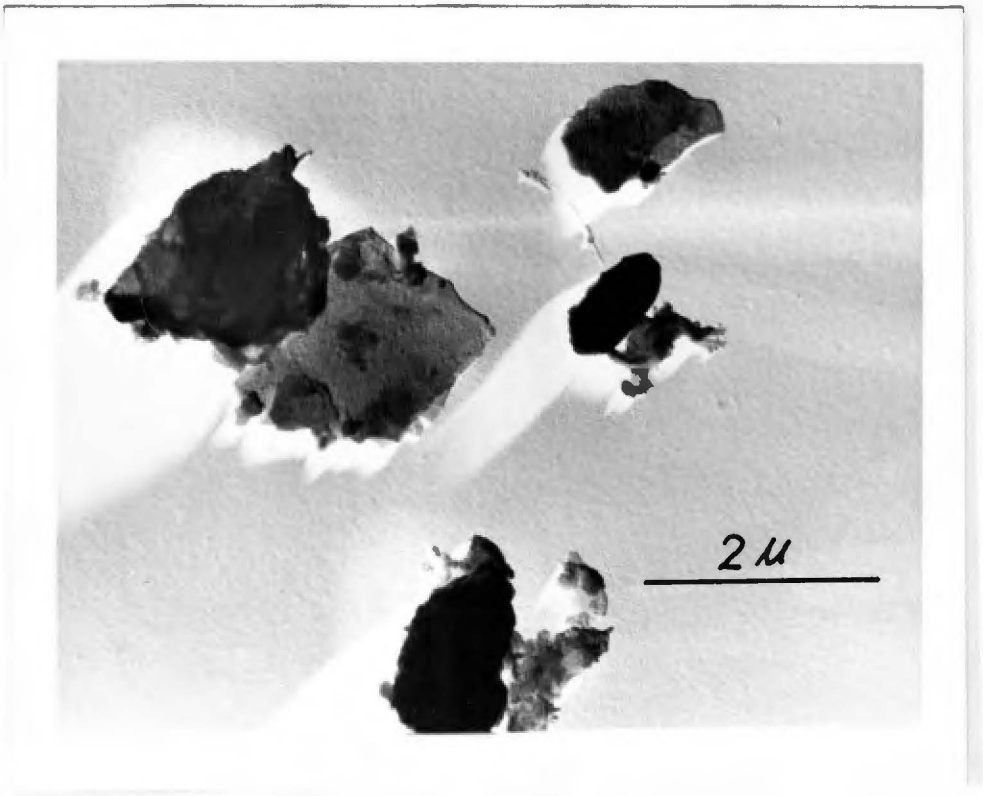

Fig. 12. Electron Micrograph of the Coarse Clay Fraction of the Kaipoioi Soil

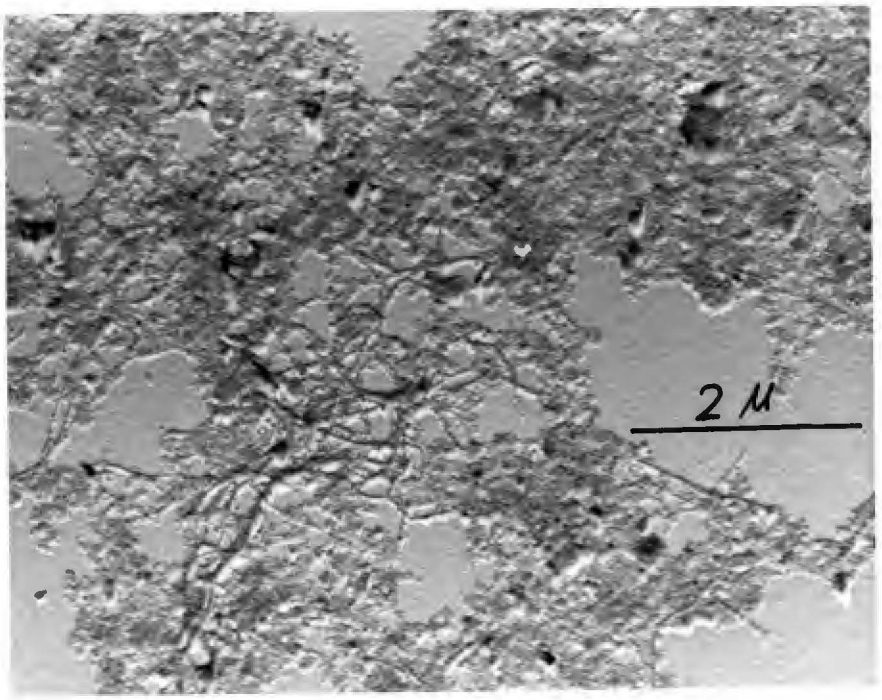

Fig. 13. Electron Micrograph of the Fine Clay Fraction of the Akaka Soil

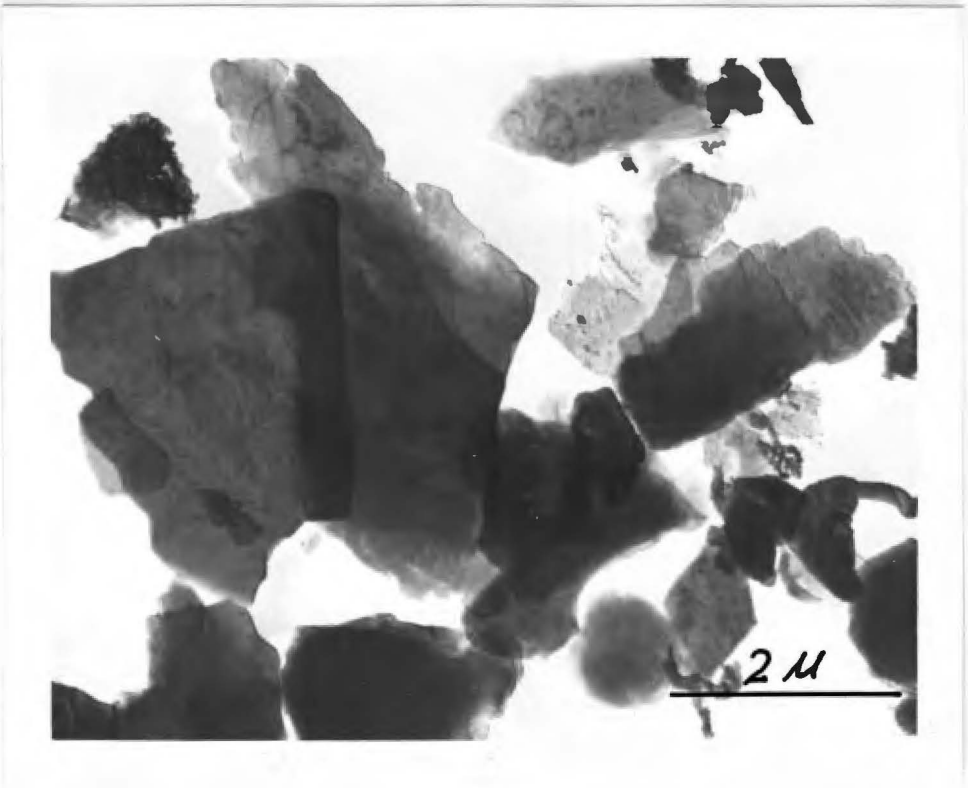

Fig. 14. Electron Micrograph of the Coarse Clay Fraction of the Akaka Soil

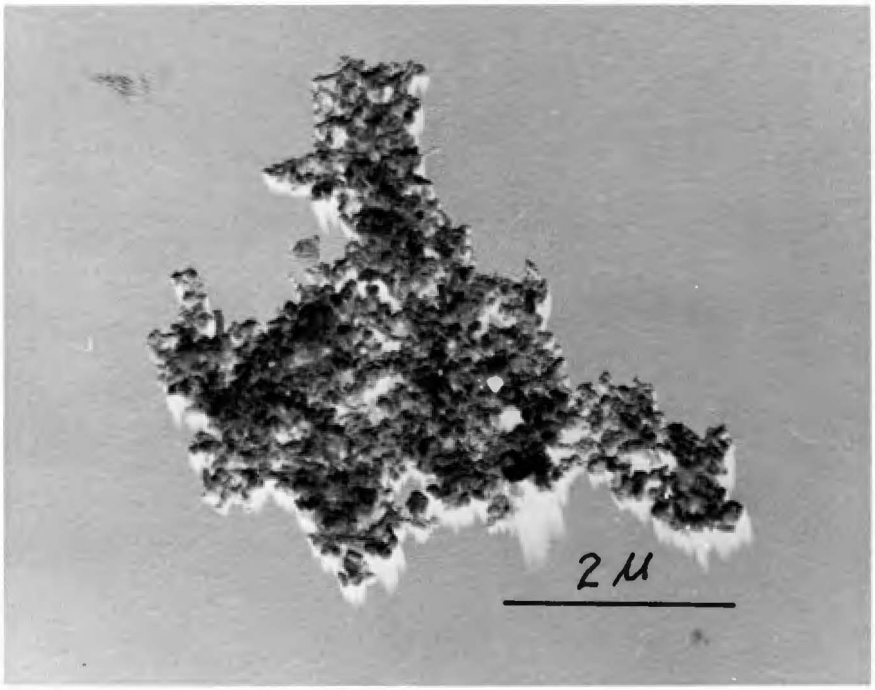

Fig. 15. Electron Micrograph of the Fine Clay Fraction of the Waikaloa Soil

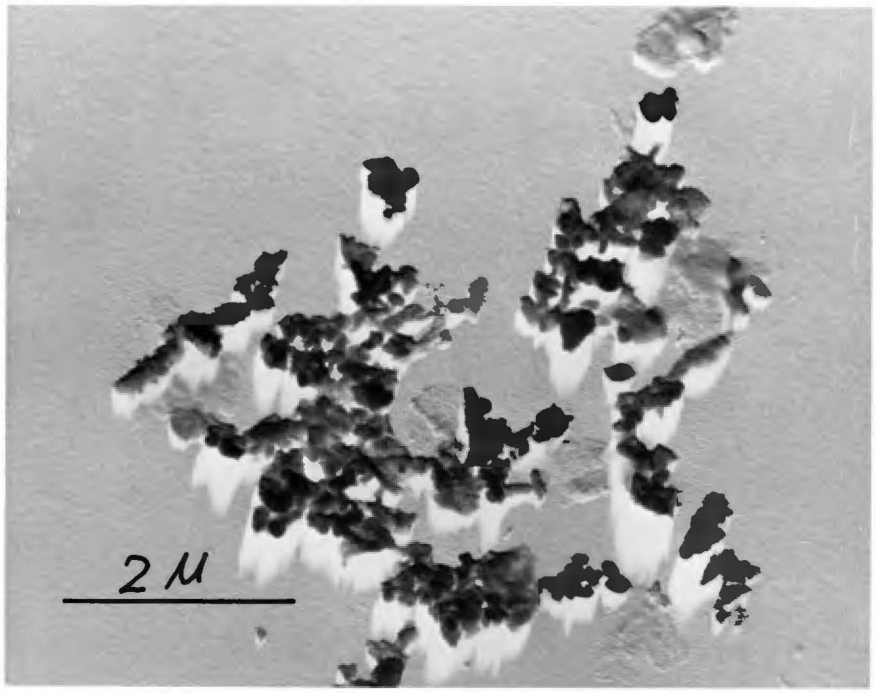

Fig. 16. Electron Micrograph of the Coarse Clay Fraction of the Waikaloa Soil

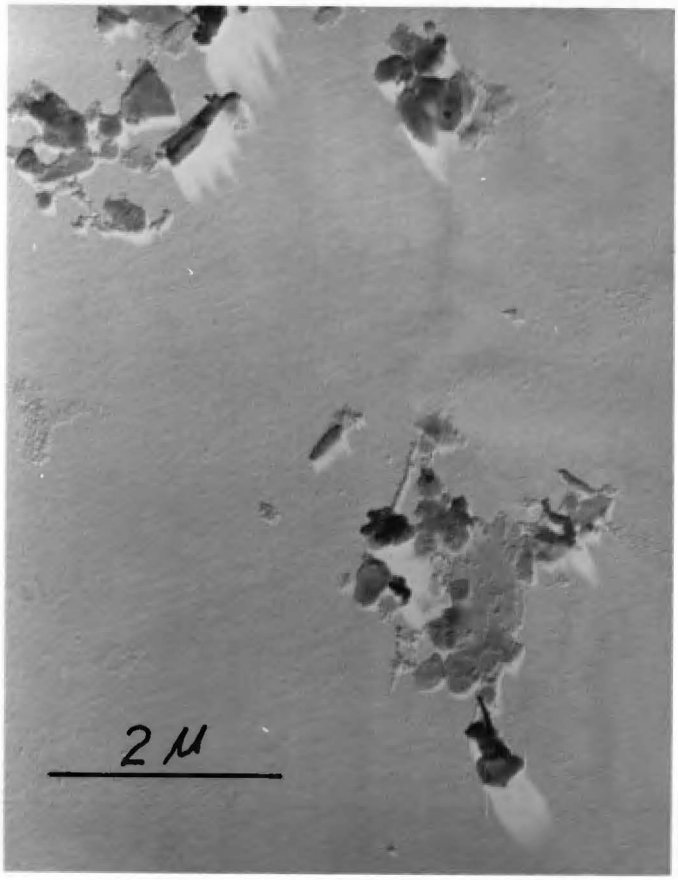

Fig. 17. Electron Micrograph of the Akaka Coarse Clay Fraction Showing Structural Defect

Fig. 18. Electron Micrograph of the Akaka Coarse Clay Fraction Showing the Moire Pattern and Structural Defect

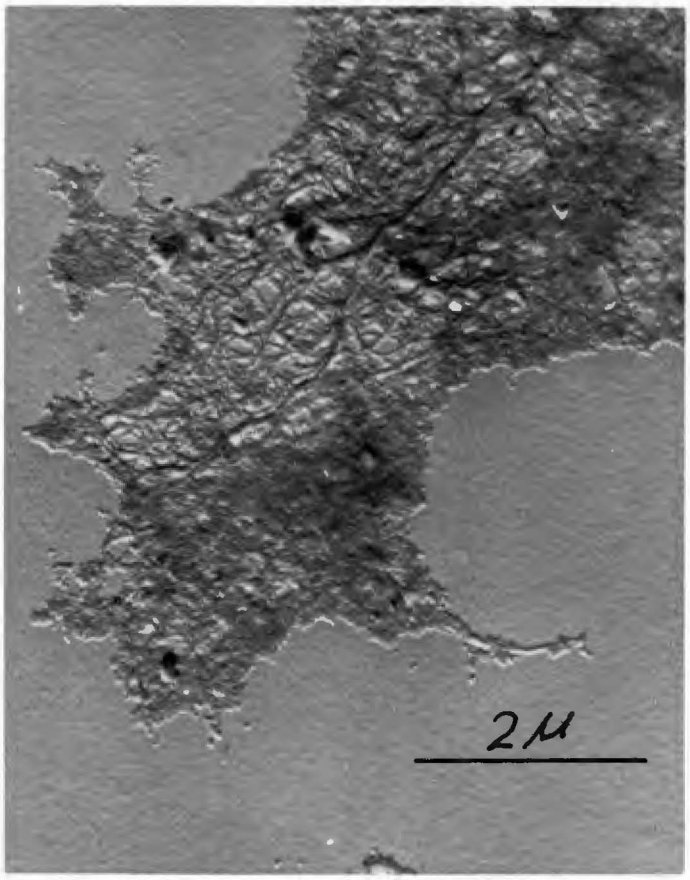

Fig. 19. Electron Micrograph of the Fine Clay Fraction of the Kealakekua Soil Showing the Interweaving of the Fibrous Network and the Sponge-like Material

Fig. 20. Electron Micrograph of the Fine Clay Fraction of the Akaka Soil Showing a Network of the Fibrous Materials

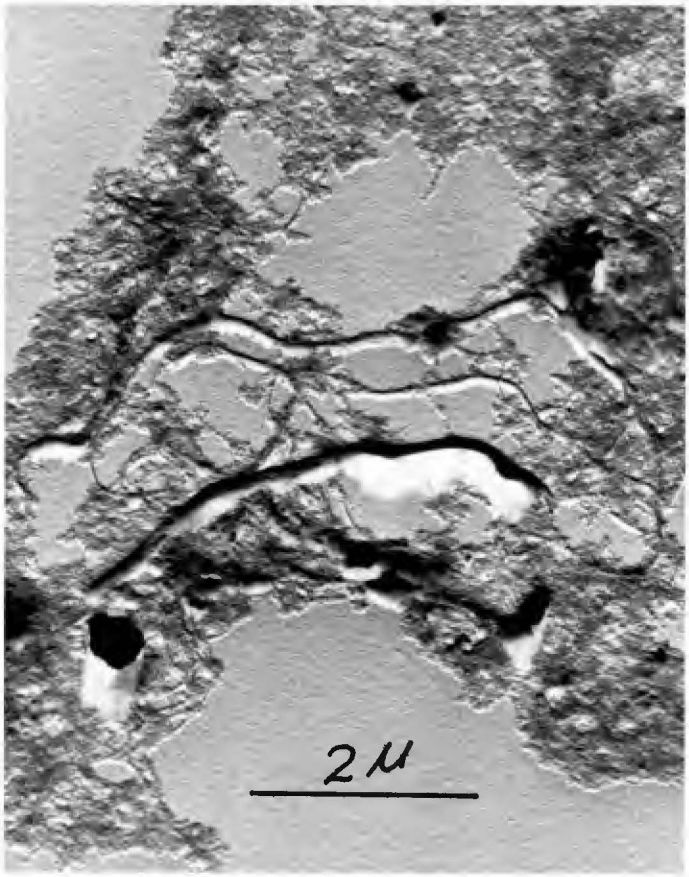

Fig. 21. Electron Micrograph of the Clay Fraction of the Kealakekua Soil Showing the Thick Threads Interconnected with the Finer Thread

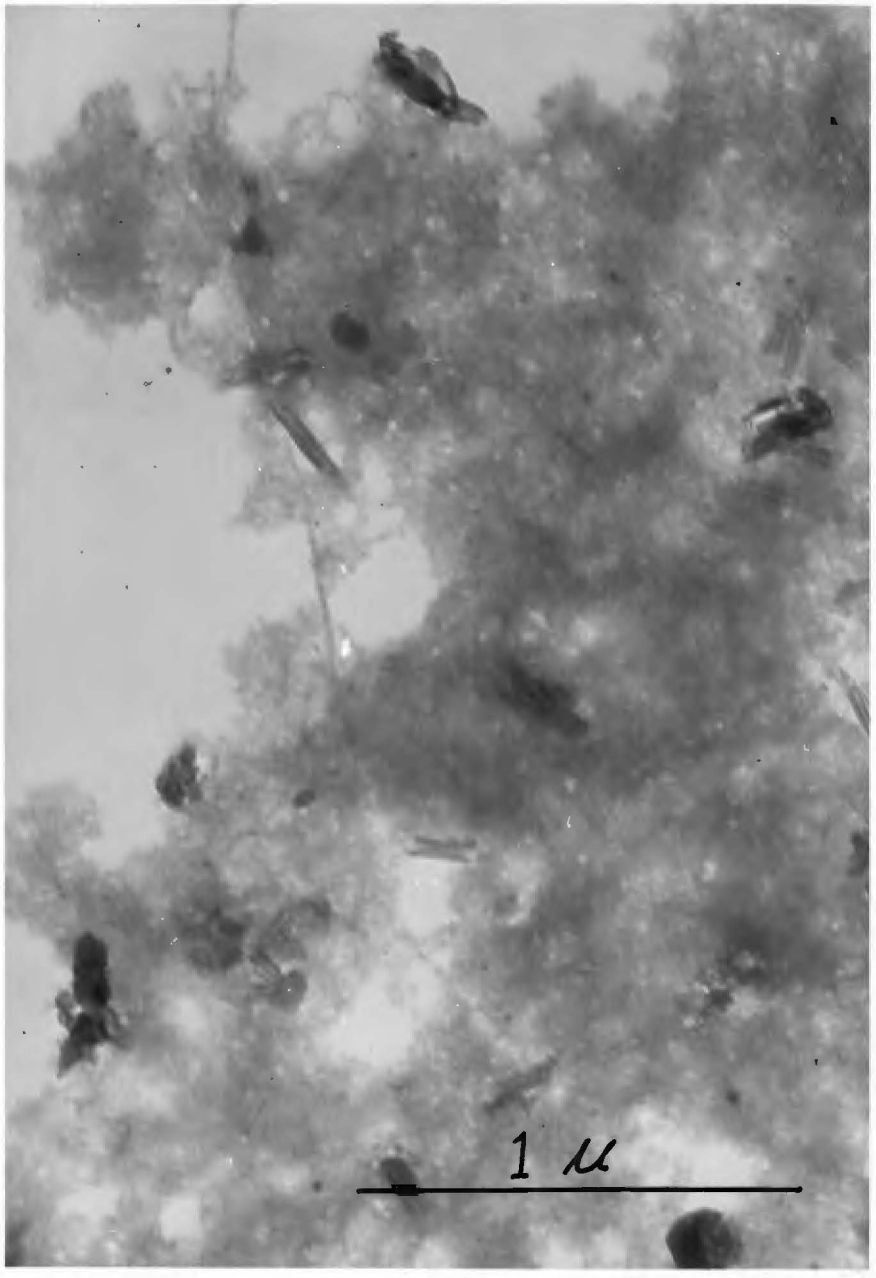

Fig. 22. Electron Micrograph Taken with Hitachi Electron Microscope. The Kealakekua Fine Clay Shows Fibrous, Sponge-like Material and the Curled Flakes or Tubes of Halloysite

Infrared Absorption Spectroscopy

The infrared (IR) absorption spectra of both the fine and coarse clay fractions are presented in Fig. 24 and Fig. 25. Before discussing the spectra of the clay samples used in this investigation, it will be desirable to observe the absorption spectra of standard halloysite which bears certain similarity to the absorption spectra of allophane.

Fig. 23 shows the absorption spectra of halloysite. The absorption peaks at 2.70, 2.73, and 2.76 μ are attributed to bound hydroxyl groups which are essential to the structure (Rich and Kunze, 1964). The diffuse bands in the regions of 2.86, 6.25 and 6.67 μ, on the other hand, are assigned to adsorbed water. The peaks at 9.01, 9.71 and 9.90 μ are due to Si-O, while the peak at 10.9 μ with a small shoulder at 10.7 μ is due to Al-H-O. The other weak peaks at 12.6 μ and the strong peak at 14.3 μ are assigned to $Si\text{-}O\text{-}Al^{VI}$, while the peak at 19.2 μ and those at 21.3 and 23.2 μ are attributable to Si-O. The main absorption bands are summarized in Table IV.

The IR spectra of Waikaloa are very similar to that of the standard halloysite. The only significant difference is the more intensive bands at 2.86 μ and 6.10 μ which indicate a greater amount of adsorbed water (Fig. 24). When the different fractions of Waikaloa are compared, the fine clay fraction shows a higher resolution of peaks between 8.33 and 25 μ. This is consistent

with the x-ray data which show more intensive halloysite peaks for the fine clay.

Akaka fine clay shows a weak peak at 2.63 μ and diffuse bands in the regions of 2.86, 6.06, 6.90 and 9.71 μ. The band between 16.7 and 25 μ resolved to peaks at 18.9, 21.3 and 23.2 μ. In the coarse clay, the band between 2.70 to 3.03 μ resolved to weak peaks at 2.76, 2.84 and 2.89 μ which resemble those of the gibbsite spectra. The band between 8.33 and 11.1 μ also resolved to weak peaks at 9.26, 9.80 and 11.0 μ. Additional weak peaks are present at 12.5, 12.8 and 14.3 μ. In general, the coarse clay shows more intensive lattice structure than the fine clay.

Kaipoioi, Kealakekua, and Choyo show very similar spectra with increasing resolution of the absorption bands between 8.33 to 25 μ.

Fieldes et al. (1956) reported that a characteristic absorption band at 12.5 μ indicates the presence of allophane B. None of the samples show this characteristic band, and this behavior supports the DTA data that allophane B is not identifiable in the samples studied.

The main Si-O absorption bands between 7.69 and 12.5 μ for fine clays were taken for a closer study. In Fig. 26, it was noticed that the absorption maxima shift is toward the longer wavelengths. Table V lists the wave number and wave length of

the maxima, and the percent by weight of Al_2O_3.

The wavelength of absorption maxima is plotted against $Al_2O_3/(Al_2O_3+SiO_2)$ in Fig. 27. As the ratio increases from 50% to 65%, the absorption maximum shifts from 9.75 μ to 10.3 μ. From the studies by Stubican and Roy (1961); De Kimpe, Gastuche and Brindley (1964); and Leonard, Suzuki, Fripiat, and De Kimpe (1964), the reasons for the shift of Si-O band are summarized as: (1) The increase of Al in the octahedral structure. (2) The increasing tendency of tetrahedral aluminum to share edges with tetrahedral silica.

At this point, it is necessary to clarify the structural features of Al in 4-coordination. Leonard et al. (1964) pointed out that there are two kinds of Al-tetrahedra: (1) Al tetrahedron with sharing corners, and (2) Al tetrahedron with sharing edges. The first type of Al^{IV} is stabilized by 4 surrounding Si tetrahedra, and the maximum amount of Al in this structural state is about 30% (Milliken, 1950). Beyond this, the Al takes 6 coordination. The second type of Al^{IV} is obtained by ignition and dehydration of the Al octahedra. Since the percent weight of Al in the samples is higher than 30% (50% or above), it is expected that the Al^{VI} will increase with increasing Al. There is possibility that Al^{IV} of the second type exists in the less weathered allophane. This will be discussed in a later section. Thus the Si-O band shift could be attributed to both the increase of Al^{VI} and the Al^{IV} of

Table IV. Position and Intensity of IR Absorption Bands for Halloysite (μ)

OH	H_2O	Si-O	Al-H-O	Si-O-Al^{VI}	Si-O	Si-O-Al^{VI}	Si-O
2.70s	6.25w	9.01s	10.9s	12.6w	14.3m	18.5s	21.3s
2.73w	6.67w	9.71s	10.7w	13.3w			23.2m
2.76m		9.90s					

s=strong m=medium w=weak

Table V. The 10.0 μ Band Shift and the Weight Percent of Al in Five Fine Clays

Soils	Wave No.	Wavelength	$Al_2O_3/(Al_2O_3+SiO_2)$
	(cm^{-1})	(μ)	(%)
Choyo	970	10.30	64.68
Kealakekua	975	10.25	64.30
Kaipoioi	990	10.10	58.69
Akaka	1020	9.80	53.07
Waikaloa	1025	9.77	52.65

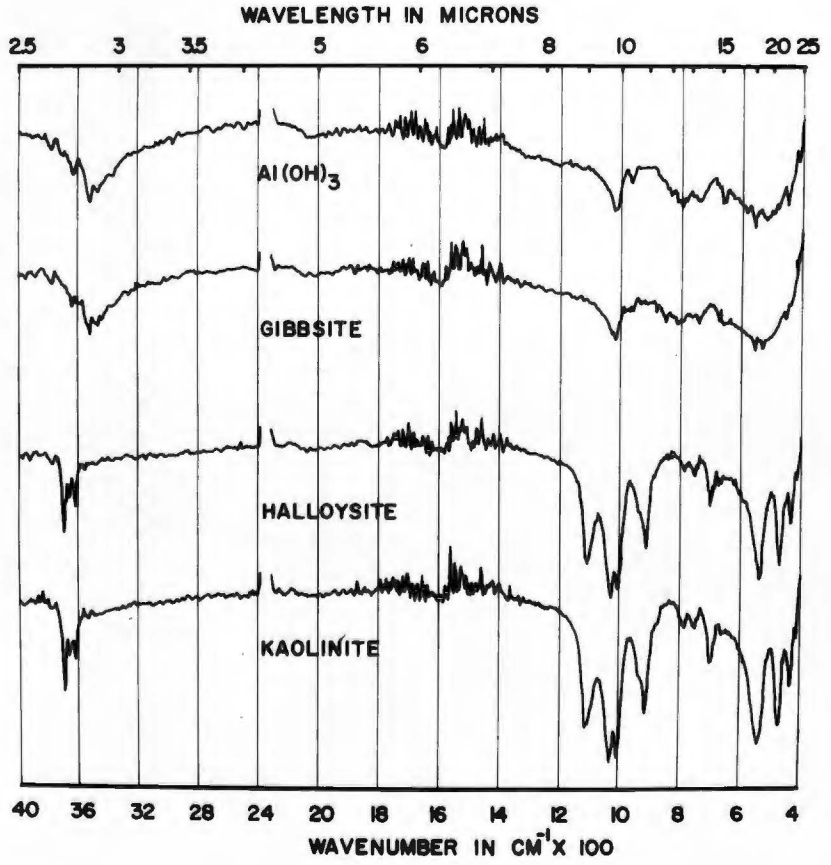

Fig. 23. Infrared Absorption Spectra of Some Standard Minerals

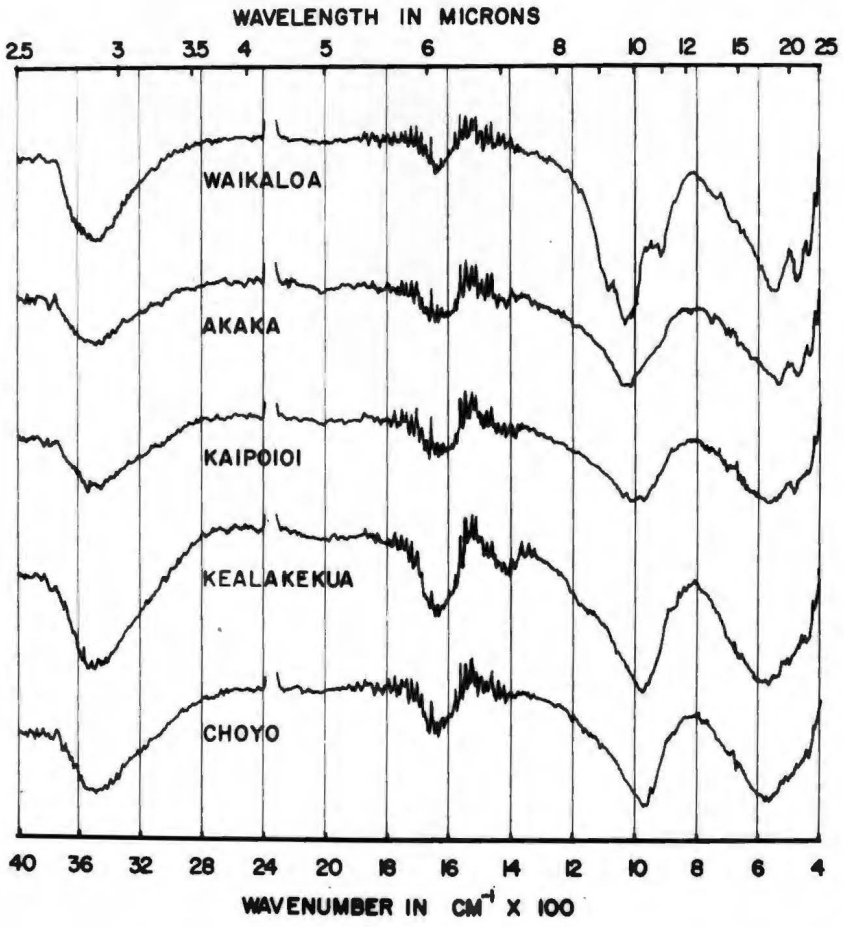

Fig. 24. Infrared Absorption Spectra of the Fine Clay Fractions

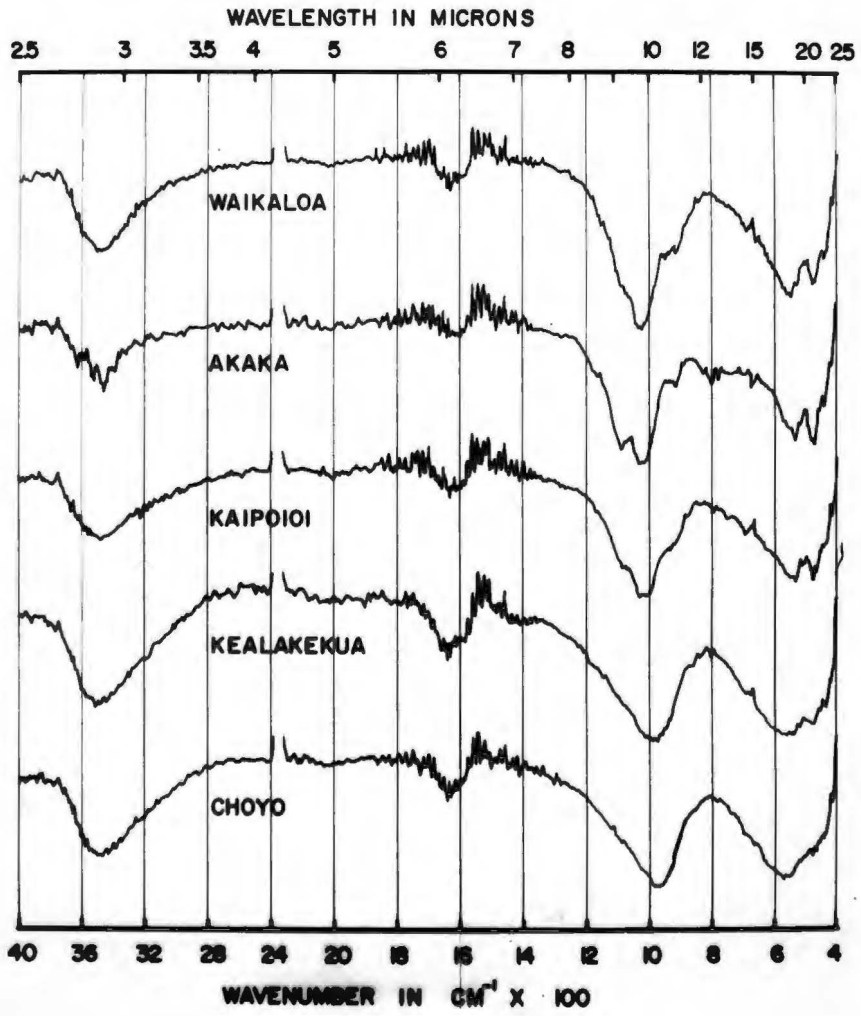

Fig. 25. Infrared Absorption Spectra of the Coarse Clay Fractions

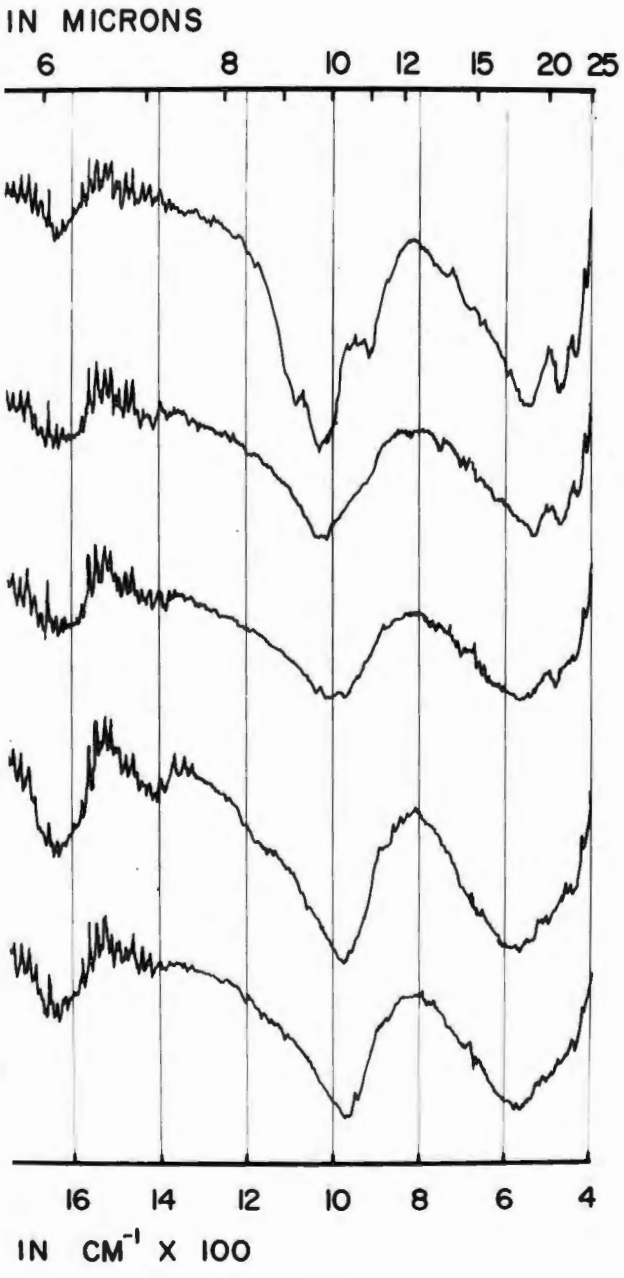

Fig. 26. Infrared Absorption Spectra Showing the 10 μ Maxima Shift. Enlargement of Fig. 24 in the Region of Interest

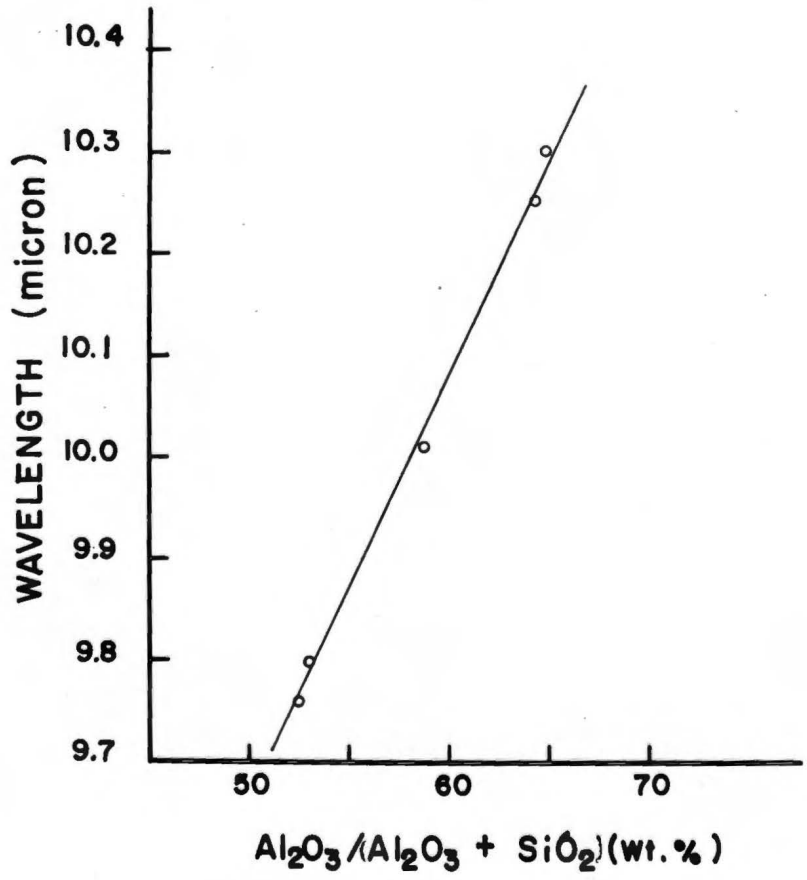

Fig. 27. The Infrared Absorption Maxima Shift at 10 μ Versus Chemical Composition

the second type. Unfortunately, the present data are not enough to separate these two factors, and the quantitative evaluation of Al^{IV} and Al^{VI} is impossible.

Surface Area

The surface areas determined are shown in Table VI.

The highly fibrous and sponge-like allophane having many empty holes leads us to expect it to have a high surface area. It is also expected that the more amorphous clay of Choyo and Kealakekua should show a higher surface area than that of Akaka and Waikaloa. However the determined values were quite different from what had been expected. In the first column of Table VI, the surface area decreases rather than increases from Waikaloa to Choyo. The values obtained from air-dried samples and wet samples also show differences.

The method was checked with standard mineral and yielded satisfactory values for kaolinite (30 m^2/g) and bentonite (720 m^2/g). The principle of this method is the coulombic adsorption of CPB molecules by the clay particles to form a monolayer of CPB. The success of this method depends on the charge density, which has to be high enough to adsorb a monolayer of CPB to completely cover the particle surface. As will be seen in the next section, the surface charge of allophane is pH dependent. The pH of the suspension system for the surface area determination was about 6.5. At this pH, the net negative

Table VI. Surface Areas Determined Before and After Air Drying for Fine and Coarse Fractions of Five Clays (m^2/g)

Soils	Fine Clay		Coarse Clay	
	Wet	Dried	Wet	Dried
Choyo	79.2	121	41.6	9.94
Kealakekua	80.7	174	98.6	93.9
Kaipoioi	109	240	73.8	73.2
Akaka	131	209	77.0	54.8
Waikaloa	147	107	120	118

charge as shown in Figs. 28 and 29 is relatively lower than that at higher pH. The charge density at this pH may not be high enough to adsorb enough CPB molecules to completely cover the surface of allophane. If the pH of this system was maintained at a higher level (e.g. 8.5), it may give higher value for the surface area. Unless a complete monolayer is assured, the CPB adsorbed cannot be taken for surface area determination.

Cation Exchange Capacity and Its pH Dependence

The change of electric charge with varying pH was investigated by determining the cation exchange capacity (CEC) at different pH's. The CEC represents the net negative charge possessed by the clay. Therefore, the CEC at different pH's reveals the change of the negative charge of a clay under different H^+ concentration.

The CEC and ΔCEC of the fine and coarse clay fractions are shown in Table VII. The relationship between CEC and pH is shown in Figs. 28 and 29. From Figs. 28 and 29, some general characteristics are summarized: (1) The negative charge increases with increasing pH, (2) The change of CEC between pH 4 and 7 is much less than that between pH 7 and 8.5, and (3) An inverse relationship exists between crystallinity and the change of CEC with pH.

The ΔCEC which is the difference of CEC between pH 4 and 8.5 was plotted against the $Al_2O_3/(Al_2O_3+SiO_2)$ weight ratio

Table VII. CEC at Four Different pH Levels for Fine and Coarse Clay Fractions of the Five Soils (me./100 g)

pH	Choyo	Kealakekua	Kaipoioi	Akaka	Waikaloa
			Fine Clay		
4.0	53.14	68.26	81.71	60.15	50.05
5.5	69.49	113.8	125.3	81.15	74.10
7.0	71.63	102.8	119.3	83.01	67.72
8.5	161.5	218.4	221.1	157.6	103.0
ΔCEC	108.3	150.2	139.4	97.48	53.00
			Coarse Clay		
4.0	25.76	43.01	38.13	25.29	56.53
5.5	47.35	72.43	58.67	30.59	74.54
7.0	64.40	78.47	58.67	30.59	75.18
8.5	159.1	178.8	108.2	44.87	106.0
ΔCEC	133.4	135.8	70.04	19.58	49.39

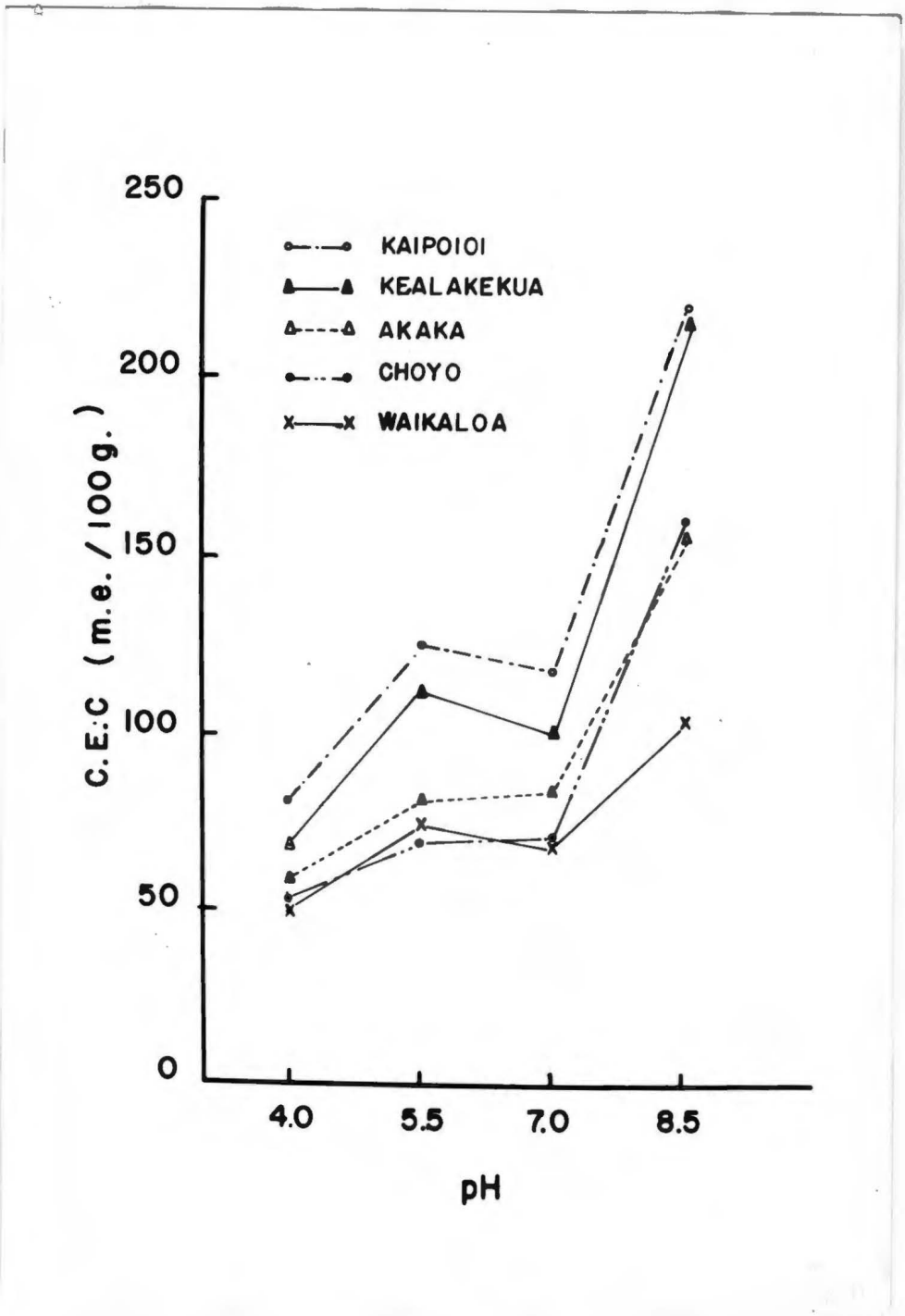

Fig. 28. The Cation Exchange Capacity of the Fine Clay Fractions at Different pH Values

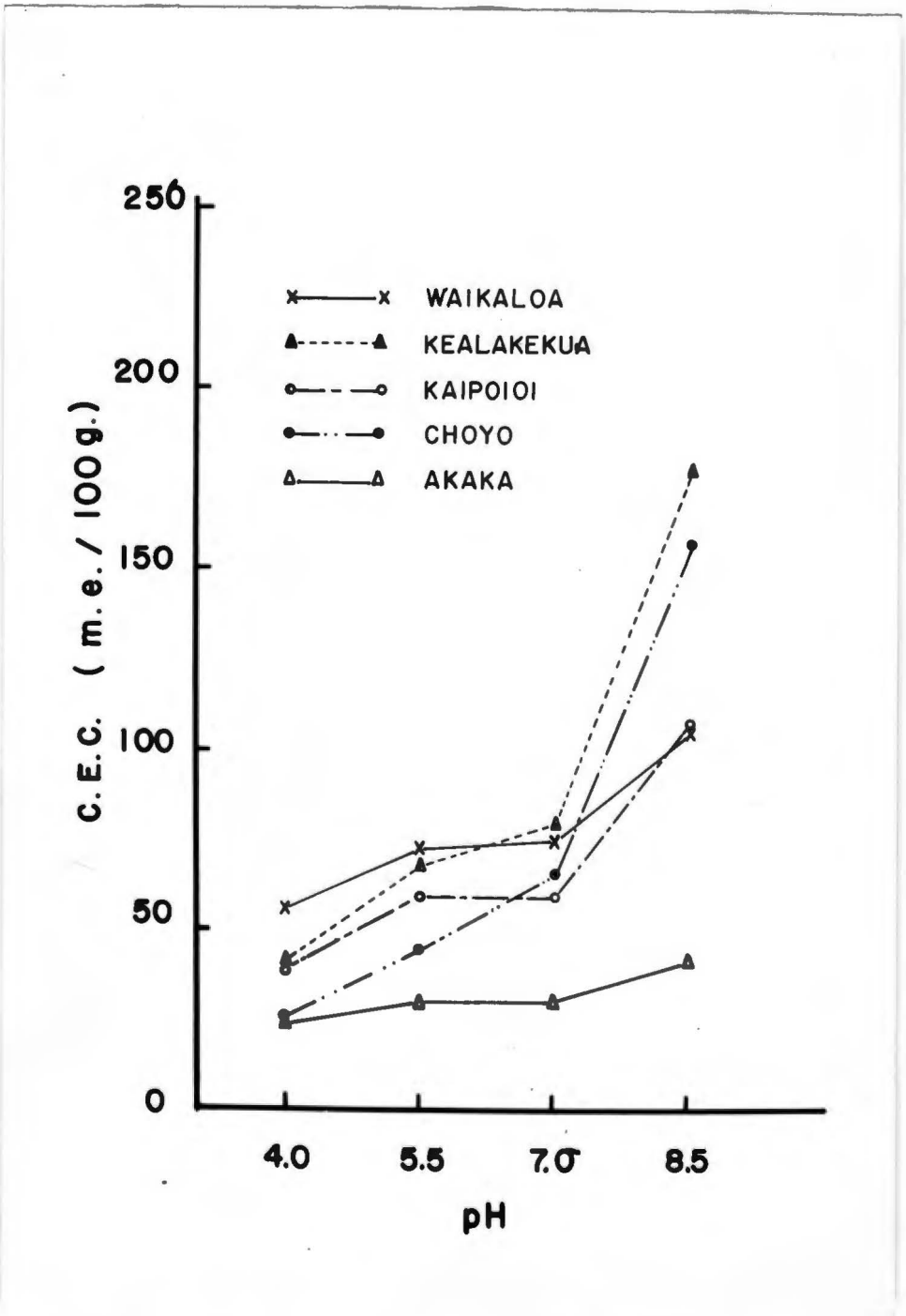

Fig. 29. The Cation Exchange Capacity of the Coarse Clay Fractions at Different pH Values

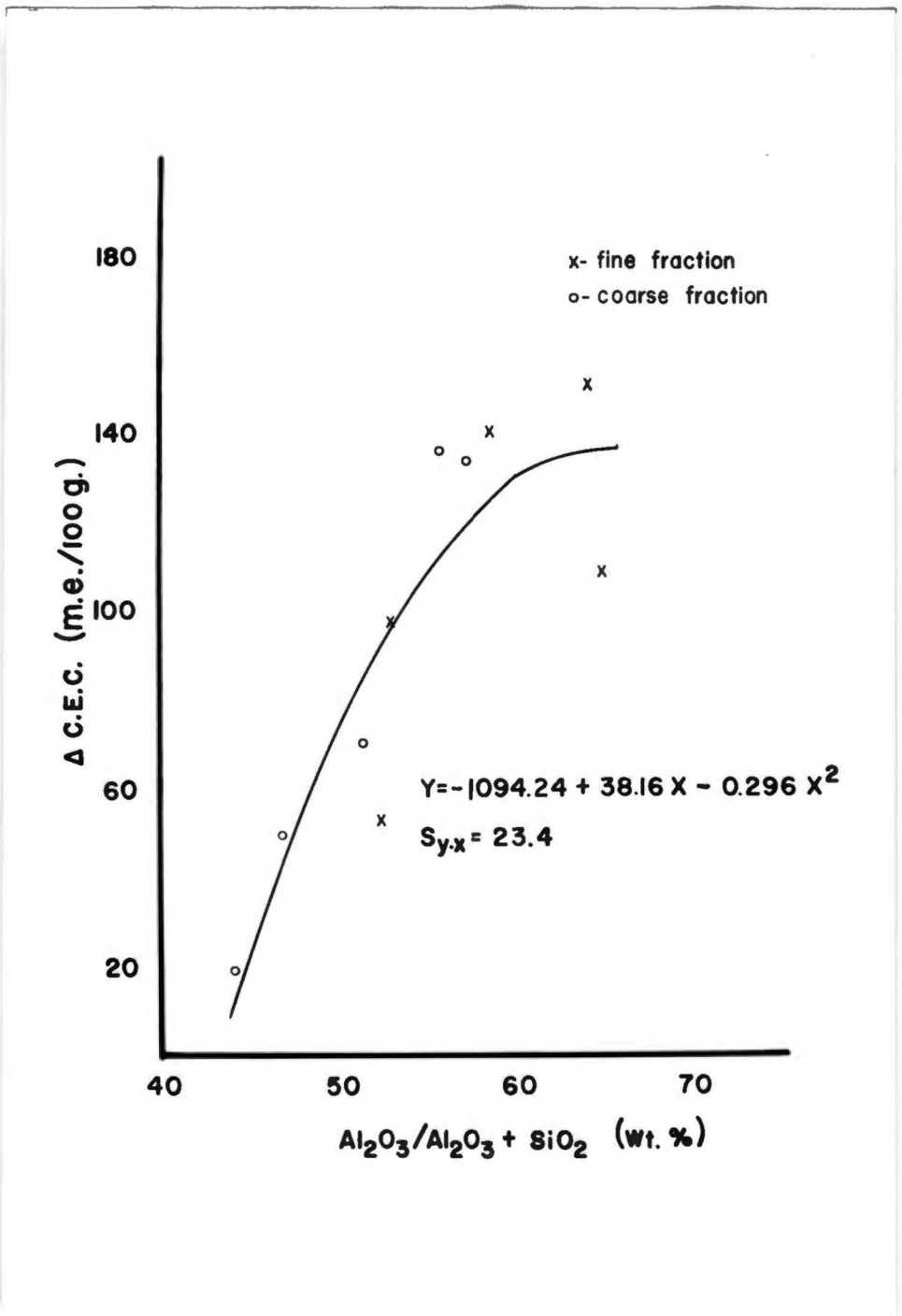

Fig. 30. The Regression of ΔCEC Versus $Al_2O_3/(Al_2O_3+SiO_2)$ Weight Percentage of the Five Clays

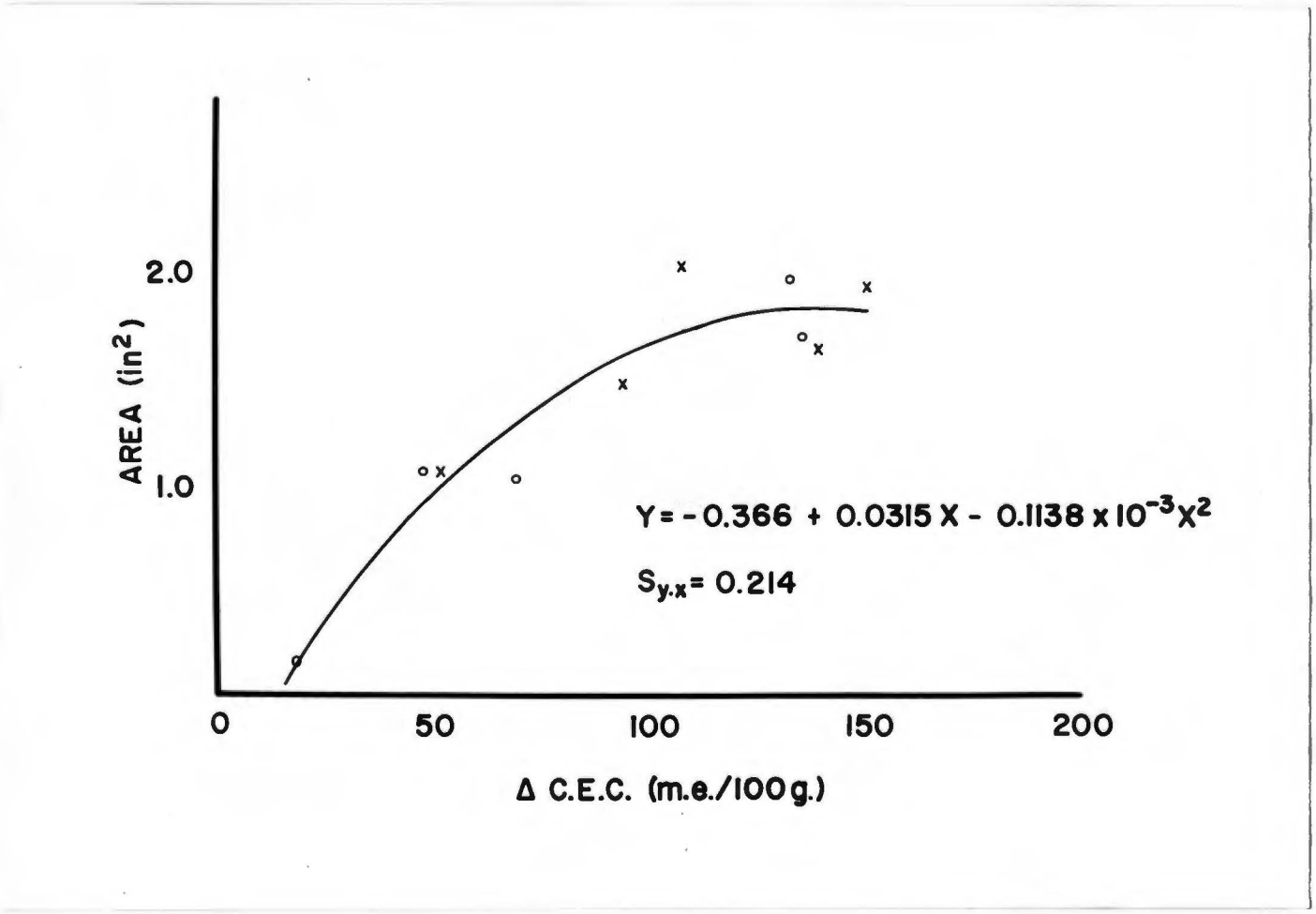

Fig. 31. The Regression of the Area of the First DTA Endothermic Peaks Versus ΔCEC of the Five Clays. See Fig. 30 for Key to Symbols Used

in Fig. 30. The ΔCEC and $Al_2O_3/(Al_2O_3+SiO_2)$ graph yields a curvilinear relationship within the Al_2O_3 weight ratio range between 40 to 65%. The ΔCEC tends to level off at the Al_2O_3 weight ratio of 65%.

The ΔCEC is also related to the adsorbed water as expressed by the first endothermic peak on the DTA pattern. The area of the first endothermic peak was plotted against the ΔCEC (Fig. 31). The graph yields a curvilinear regression between the peak area and the ΔCEC.

Houng et al. (1966) concluded that the charges of allophanic clay were mostly due to the surface silanol groups and tetrahedrally coordinated aluminum atoms. In this study, it is known that the ΔCEC increases curvilinearly with $Al_2O_3/(Al_2O_3+SiO_2)$ ratio and tends to level off at 65% of the ratio. It seems that the pH dependent charge depends more on Al than on Si. It is known that as the amount of 4-coordinated aluminum increases, the charge originating from the isomorphous substitution of Al for Si also increases. Other things being equal, it is supposed that the higher CEC indicates a higher concentration of 4-coordinated Al. Milliken et al. (1950) and De Kimpe et al. (1961) pointed out that in synthetic silico-alumina gel, the 4-coordinated Al reaches a maximum when the weight ratio of $Al_2O_3/(Al_2O_3+SiO_2)$ is at 30%. De Kimpe also determined the CEC of the silico-alumina gel and found its maximum CEC at 20% $Al_2O_3/(Al_2O_3+SiO_2)$. However,

Houng (1964) obtained the same maximum at 42%. Houng et al. (1966) also found that the maximum amount of tetrahedral Al in the silico-alumina gel can be as high as 62% instead of 50% as determined by Iler (1955). There is, therefore, reason to doubt that the synthetic silico-alumina gel can be relied on to depict the structure and properties of naturally-occurring allophane. A comparison of the IR data shows that the main absorption band of the Si-O for the synthetic silico-alumina of various Al^{IV} concentration is between 9.9 and 9.1 μ. However, the same data obtained for allophane in this study lie between 10.3 and 9.8 μ. This dissimilarity indicates that there may be structural differences between synthetic silico-alumina and naturally-occurring allophane. The longer wavelength of the Si-O band in allophane implies a weaker bonding or higher randomness of the Si tetrahedral structure and its isomorphous equivalent. This may provide more opportunity for Al to be in the tetrahedral structure.

It is speculated that even under a $Al_2O_3/(Al_2O_3+SiO_2)$ ratio higher than 30% in allophane, the relative amount of Al in 4-coordination is higher, and the charge due to this Al^{IV} is higher than that in synthetic silico-alumina. Therefore, it is suspected that in addition to the structure (A) there may be some Al taking the (B) form as shown on the following page.

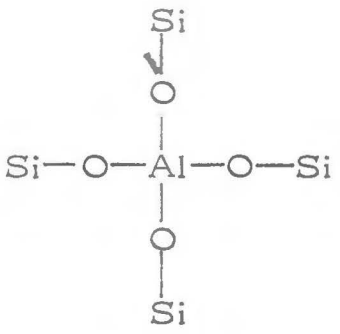

Form (A)

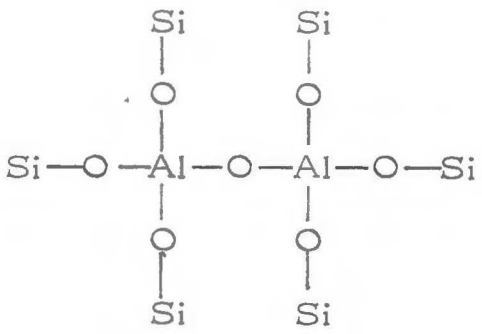

Form (B)

This structure will probably cause the system to possess high free energy increasing the tendency of Al^{IV} to change to the stable form of Al^{VI}. Therefore allophane tends to change to halloysite, provided there is available H_4SiO_4, and Al^{VI} will ultimately be obtained.

Houng et al. (1966) has pointed out that the charge due to isomorphous replacement can be pH-dependent or permanent, depending on the distance between the surface of the exchanger and the site where the isomorphous replacement occurs. The extremely small size of allophane makes this distance very short when compared with crystalline minerals. The charges so initiated produce a strong polarizing effect on the hydronium ions and promote the formation of hydroxyl groups on the clay particles. This charge is therefore pH-dependent.

Overall Evaluation by Sample

From the foregoing discussion of the results obtained, it is clear that besides the Waikaloa and the coarse clay of Akaka, all the samples are predominantly allophanic. The results are

summarized with respect to each sample and then compared with whatever results of each sample as are available in previous literature.

Waikaloa

DTA, IR data and electron micrographs clearly indicate that the predominant secondary mineral in this soil is halloysite. A certain amount of allophane is also present. Tenma (1965) reported 12% allophane on a whole soil basis. The SiO_2/Al_2O_3 ratios for the fine and coarse clay fractions are 1.53 and 2.14 respectively. The CEC at pH 7 for the fine and coarse clay fractions are 67.7 and 75.2 me./100 g respectively. Tenma reported a ratio of 2.09 for the clay fraction. The high value of ΔCEC for both fine and coarse clays as seen in Table VII indicates that halloysite also possesses a fairly high pH-dependent charge. This charge although less than allophane, may be greater than that of kaolinite, indicating that the pH-dependent charge decreases with an increase of weathering.

From the results obtained, it is believed that the fine clay fraction contains a larger quantity of halloysite than the coarse clay fraction. The halloysite crystals in this soil are rather weakly formed and small in size, as seen in the electron micrographs.

Akaka

Large differences exist between the fine clay and coarse clay fractions of this soil. The x-ray diffraction pattern (Fig. 2) of

the fine clay shows a band at the 16 to 10 Å region. This indicates the presence of some 2:1 minerals or interlayered minerals such as vermiculite, montmorillonite and chlorite. All these are very weakly formed if they are present. Electron micrographs and IR data also show high allophane content in this fraction. However, the coarse clay fraction has a high degree of crystallinity. The minerals were identified as mica, kaolin, gibbsite and quartz. Many larger sized flakes displaying clear Moiré pattern and well formed pseudohexagonal plates can be seen in the electron micrographs (See Figs. 14 and 18).

Tenma (1965) reported the SiO_2/Al_2O_3 ratio for Akaka clay as 0.99. In this study the value for the fine and coarse clay fractions are 1.50 and 1.94 respectively, which are significantly higher than the values Tenma reported. His x-ray diffraction pattern showed only appreciable gibbsite, without mica or kaolin which were identified in this work. This difference could be due to variation of the samples and different methods of clay separation. The sample used in this study was collected by Kanehiro (1965).

The CEC at pH 7 for fine clay and coarse clay fraction are 83.0 and 30.6 me./100 g respectively. The drastic difference in ΔCEC for these fractions (Table VII) indicates that the fine clay has a high allophane content, while the coarse clay contains predominantly crystalline minerals.

Kaipoioi

Both the fine and coarse clay fractions of the Kaipoioi show a resemblance to the Akaka in their composition. Comparing x-ray (Figs. 2 and 3) and electron micrographs (Figs. 12 and 14), it is clear that Kaipoioi is weaker in crystallinity than the Akaka. The fine fraction shows a weak band between 20 to 10 Å, indicating weakly formed 2:1 and interlayered minerals and a large amount of allophane.

The coarse clay fraction shows a mica and kaolin x-ray diffraction pattern. The electron micrograph of the same fraction occasionally display well formed flakes which could very well be mica or kaolin (Fig. 12).

The SiO_2/Al_2O_3 ratios for both the fine and coarse clay fractions are higher than that reported by Tenma (1965). Comparing Table I and Table III, the difference could be due to the procedure for sample pretreatment, dispersion, and separation. Tenma did not boil the soil with 2% Na_2CO_3 before dispersion. This boiling may bring more crystalline clay mineral into dispersion and hence included in the separation. The CEC at pH 7 and ΔCEC are higher than that for the Akaka (Table VII). All the results are consistent and show that the Kaipoioi has a higher allophane content than the Akaka.

Kealakekua

The Kealakekua has the highest allophane content among the Hawaiian soils included in this study. It shows a very close resemblance to the Choyo, particularly the fine clay fraction. The coarse clay does show a higher degree of crystallinity than the Choyo with an appreciable amount of weakly formed mica, kaolin and gibbsite as identified from the x-ray diffraction pattern (Fig. 3). This soil has SiO_2/Al_2O_3 ratios of 0.94 and 1.35 for the fine and coarse fractions respectively. The ratio determined by Tenma (1965) for the clay fraction was 0.96. Kealakekua has the highest ΔCEC among the five samples studied here (See Table VII). It is suspected that this sample possesses the highest pH-dependent charge and a further increase of Al will not increase the ΔCEC according to Fig. 30.

Considering all the results obtained for this sample, it is summarized that the fine fraction of the Kealakekua soil contains almost pure allophane.

Choyo

The resemblance of Choyo and Kealakekua has been mentioned. Choyo is the least crystallized sample of all the soils studied. Even the coarse clay fraction does not show any clear x-ray diffraction peaks, aside from some weak bands (Fig. 3). The electron micrographs and IR data in this study are comparable to that reported by Yoshinaga and Aomine (1962).

The SiO_2/Al_2O_3 ratio of the clays is the lowest among all the samples, i.e., the Al content is the highest. The ΔCEC is, however, slightly less than that of the Kealakekua. It is believed that the Al^{VI} in the Choyo is higher than that of the Kealakekua. These results also support the belief that Choyo clay is pure allophane.

SUMMARY AND CONCLUSION

This thesis has dealt with the investigation of certain soils of volcanic ash origin which were moderately to strongly weathered. One sample, Choyo, was obtained from Japan, while the remaining four were from Hawaii.

Mineral colloids were separated from the soil samples in alkaline and acid media by the particle size method.

The study was concentrated on the fine clay fraction (less than 0.1 μ) which was separated in the alkaline media and considered mainly allophane. The coarse clay fractions (2-0.1 μ) from each sample were, for the most part, crystalline. The mineral colloids were examined by several physical-chemical methods: X-ray diffraction analysis, differential thermal analysis, elemental analysis, electron microscopy, infrared absorption spectroscopy, surface area determination. The results are summarized as follows:

1. X-ray diffraction analysis showed that fine clay is x-ray amorphous with various amounts of weakly formed 2:1 minerals except in the case of Waikaloa. The coarse clay fraction consisted mainly of crystalline minerals, mica, kaolin, and gibbsite.
2. Differential thermal analysis of the fine clay fraction showed a strong endothermic peak between 100°C. and

150°C. and an exothermic peak between 850°C. and 950°C. The area of the first endothermic peak was closely related to the degree of crystallinity as determined by x-ray diffraction methods.

3. Elemental analysis indicated that the SiO_2/Al_2O_3 molar ratios for fine and coarse clay fractions were 0.927 to 1.527 and 1.260 to 1.940 respectively. The loss on ignition was inversely proportional to the SiO_2/Al_2O_3 ratio.

4. The electron micrographs showed fibrous and sponge-like features in the fine clay fraction. Such observations suggest the transformation of allophane to crystalline alumino-silicates. As crystallinity increased, the morphology of the clay particles changed from irregularly shaped flakes to pseudohexagonal flakes. This change is accompanied by an increase in the size of the flakes as shown in the coarse fraction.

5. The infrared absorption spectra of amorphous mineral colloids generally showed a similarity to those of alumino-silicates. The main absorption band at 10 μ shifted from 9.75 μ to 10.3 μ as the $Al_2O_3/(Al_2O_3+SiO_2)$ weight ratio increased from 50% to 65%. This reflects a change in the coordination state of alumina.

6. The results of the surface area determinations are inconsistent with the conclusions obtained from the observations of the electron micrographs.

7. The CEC generally increased as pH increased, especially on the alkaline side. The ΔCEC increased curvilinearly with the $Al_2O_3/(Al_2O_3+SiO_2)$ weight ratio from 45% to 65%. This may be attributed to the strong acidic behavior of Al^{IV}.

SUGGESTIONS FOR FUTURE WORK

1. Investigate the effect of sodium carbonate boiling on the dispersion of allophanic clays.
2. Study the transformation of allophane to halloysite, mica, and gibbsite by using electron microscopy and electron diffraction techniques.
3. Develop a suitable method for determining surface areas of amorphous clays.
4. Determine the coordination of aluminum quantitatively.

LITERATURE CITED

1. Aomine, S., and Miyauchi, N. 1965. Imogolite of Imogo-layers in Kyushu. Soil Sci. and Plant Nutr. 11:212-219.

2. Aomine, S., and Yoshinaga, N. 1955. Clay minerals of some well-drained volcanic ash soils in Japan. Soil Sci. 79:349-358.

3. Beutelspacher, H., and van der Marel, H. W. 1961. Uber die amorphen Stoffe in den Tonen verschiedener Boden. ACTA Universitatis Caroline, Geo. Suppl. 1:97-114.

4. Birrell, K. S. 1964. Some properties of volcanic ash soils. Report on the "Meeting on the Classification and Correlation of Soils from Volcanic Ash". World Soil Resources Report No. 14. FAO, Rome, 1965.

5. Birrell, K. S., and Fieldes, M. 1952. Allophane in volcanic ash soils. J. Soil Sci. 3:157-166.

6. Birrell, K. S., and Gradwell, M. 1956. Ion-exchange phenomena in some soils containing amorphous mineral constituents. J. Soil Sci. 7:130-147.

7. Bunting, W. E. 1944. The determination of soluble silica in very low concentration. Indus. Eng. Chem. Anal. Ed. 16:612-615.

8. De Kimpe, C., Gastuche, M. C. and Brindley, G. W. 1961. Ionic coordination in alumina-silicate gels in relation to clay mineral formation. Amer. Mineral. 46:1370-1381.

9. De Kimpe, C., Gastuche, M. C., and Brindley, G. W. 1964. Low-temperature syntheses of kaolin minerals. Amer. Mineral. 49:1-16.

10. Egawa, T. 1964. Nature and properties of allophane. Report on the "Volcanic Ash Soils in Japan". Tokyo, 1964.

11. Egawa, T. 1964a. Mineralogical properties of volcanic ash soils in Japan. Report on the "Meeting on the Classification and Correlation of Soils from Volcanic Ash". World Soil Resources Report No. 14, FAO, Rome, 1965.

12. Egawa, T. 1964b. A study on coordination number of aluminum in allophane. Clay Sci. 2:1-7.

13. Fieldes, M. 1955. Clay mineralogy of New Zealand soils, Part 2: Allophane and related minerals. N. Z. J. Sci. Techn. 37:336-350.

14. Fieldes, M., Walker, I. K. and Williams, P. P. 1956. Clay mineralogy of New Zealand soils, Part 3: Infrared absorption spectra of soil clays. N. Z. J. Sci. Techn. 38:32-43.

15. Gorcey de Longuyen, J. 1958. Ber. Deutsch Keram. Ges. 38:155-158.

16. Greenland, D. J., and Quirk, J. P. 1960. Adsorption of 1-n-alkyl pyridinium bromide by montmorillonite. Clays and Clay Min. 9:484-499.

17. Greenland, D. J., and Quirk, J. P. 1962. Surface areas of soil colloids. Trans. Comm. IV and V, Int. Soc. Soil Sci. New Zealand, 79-87.

18. Greenland, D. J., and Quirk, J. P. 1964. Determination of the total specific surface areas of soils by adsorption of cetyl pyridinium bromide. J. Soil Sci. 15:178-191.

19. Grim, R. E. 1953. Clay Mineralogy. McGraw-Hill Book Co., N. Y.

20. Haine, M. E., and Cosslett, V. E. 1961. The Electron Microscope. E. & F. N. Spon, Ltd., London.

21. Houng, K. H. 1964. Doctor of Philosophy Thesis. University of Hawaii, Honolulu, Hawaii.

22. Houng, K. H., Uehara, G., and Sherman, G. D. 1966. On the exchange properties of allophanic clays. (In Press)

23. Iler, R. K. 1955. The Colloid Chemistry of Silica and Silicates. Cornell University Press.

24. Jackson, M. L. 1956. Soil Chemical Analysis--Advanced Course. Published by Professor M. L. Jackson, Madison, Wisconsin.

25. Jackson, M. L. 1958. Soil Chemical Analysis. Prentice Hall, Englewood Cliffs, N. J.

26. Jackson, M. L. 1963. Aluminum bonding: A unifying principle in soil science. Soil Sci. Soc. Amer. Proc. 27:1-10.

27. Kanehiro, Y. 1965. Associate Professor, Dept. of Agronomy and Soil Science, University of Hawaii, Honolulu, Hawaii.

28. Leonard, A., Suzuki, S., Fripiat, J. J., and De Kimpe, C. 1964. Structure and properties of amorphous silicoaluminas. I. Structure from X-ray fluorescence spectroscopy and infrared spectroscopy. J. Phys. Chem. 68:2608-2617.

29. Milliken, T. H., Mills, G. A., and Oblad, A. G. The chemical characteristics and structure of cracking catalysts. Farad. Soc. Disc. 8:279-290.

30. Mitchell, B. D., and Farmer, V. C. 1962. Amorphous clay minerals in some Scottish soil profiles. Clay Min. Bull. 5:128-144.

31. Ohmasa, M. 1964. Genesis and morphology of volcanic ash soils. Report on the "Meeting on the Classification and Correlation of Soils from Volcanic Ash". World Soil Resources Report No. 14, FAO, Rome, 1965.

32. Pratt, P. F. 1961. Effect of pH on the cation-exchange capacity of surface soil. Soil Sci. Soc. Amer. Proc. 25:96-98.

33. Rich, C. I., and Kunze, G. W. 1964. Soil Clay Mineralogy: A Symposium. The Univ. of North Carolina Press, Chapel Hill, N. C.

34. Russell, E. W. 1961. Soil Conditions and Plant Growth. Wiley and Sons, Ltd., N. Y.

35. Schofield, R. K. 1949. Effect of pH on electric charges carried by clay particles. J. Soil Sci. 1:1-8.

36. Shapiro, L., and Brannock, W. W. 1962. Rapid Analysis of Silicate Rocks. Geo. Survey Bull. 1036-c. U. S. Government Printing Office, Wash., D. C.

37. Stubican, V. and Roy, R. 1961. Isomorphous substitution and infrared spectra of the layer lattice silicates. Amer. Mineral. 46:32-51.

38. Sudo, T. 1953. Clay Min. Bull. 2:96.

39. Sumner, M. E. 1963. Effect of iron oxides on positive and negative charges in clays and soils. Clay Min. Bull. 27:217-226.

40. Swindale, L. D. 1961. Bauxite in the red-brown loam soils of New Zealand. Report on "Bauxite Deposits in Northland". New Zealand Dept. Sci. and Indus. Res. Info. Series 32.

41. Swindale, L. D. 1964. The properties of soils derived from volcanic ash. Report on the "Meeting on the Classification and Correlation of Soils from Volcanic Ash". World Soil Resources Report No. 14, FAO, Rome, 1965.

42. Swindale, L. D., and Sherman, G. D. 1964. Hawaiian soils from volcanic ash. Report on the "Meeting on the Classification and Correlation of Soils from Volcanic Ash". World Soil Resources Report No. 14, FAO, Rome, 1965.

43. Tenma, H. 1965. Master's Thesis. Dept. of Agronomy and Soil Science, University of Hawaii, Honolulu, Hawaii.

44. White, W. A. 1953. Allophane from Lawrence County, Indiana. Amer. Mineral. 38:634-642.

45. Wiklander, L. 1964. Cation and anion exchange phenomena, Chemistry of the Soil. Edited by F. E. Bear. Reinhold Publishing Corporation, N. Y.

46. Yoshinaga, N., and Aomine, S. 1962. Allophane in some Ando soils. Soil Sci. and Plant Nutr. 8:6-13.